# Report on a Helicopter-Borne Magnetic Gradiometer, VLF-EM & Radiometric Survey

**Project Name:** Ida Oro
**Project Number:** 2010-007

**Client:** RYAN GOLD INC.

**Contractor:** CMG Airborne

**Date:** October 23rd, 2010

# Table of Contents



# Table of Figures

## List of Tables



## List of Appendices

## 1.0 Introduction

Canadian Mining Geophysics Ltd. (CMG) has flown a helicopter-borne magnetic gradiometer, VLF-EM & radiometric survey for Ryan Gold Inc. near Dawson City, YK.

The survey, consisting of a total of 1300 line-kilometers (l-km) and was flown September 10th to the 14th, 2010.

The survey was flown using the WGS-84 Datum and UTM Projection, Zone 8 North. The final database was converted to the NAD-83 Datum and UTM Projection, Zone 8 North using Geosoft Oasis Montaj. All map products were processed and are presented in the NAD-83 Datum.

The CMG magnetic gradiometer consists of three (3) potassium magnetometer sensors separated approximately three (3) meters (m) apart. Measured gradients include the vertical and transverse (cross-line) horizontal. The parallel (in-line) horizontal gradient is calculated and is possible because of the close separation of the magnetometer readings (~3 m) along the flight line.

The CMG system also records two VLF-EM measurements from approximately orthogonal VLF transmitting stations – normally Cutler, Maine and Jim Creek, Seattle, both in the United States.

This report describes the Property in Section 2.0, Property Geology in Section 3.0, Survey Procedures & Personnel in Section 4.0, Equipment in Section 5.0, Deliverables in Section 6.0, Processing in Section 7.0 and Results in Section 8.0.

Appendix A contains a list of the survey outline points in NAD-83, Zone 8 N.

Appendix B contains a list of the digital database columns, the database of which is included with this report to Ryan Gold Inc.

## 2.0 Property Description

The Ida Oro property is located about 90 kilometres east of Dawson City (Figure 1), in west-central Yukon. The survey polygon covers a number of mineral claims which are contiguous (Figure 2). The block is centered at latitude 64° 09′ 08″ & longitude 137° 39′ 37″. The area is on rugged terrain with elevations ranging from 750 to 1,500 meters.

The base of operations was the Eldorato Hotel, Dawson City, YK which was located about 90km west of the Ida Oro survey area. The aircraft was fueled out of a mobile slip tank stationed in near proximity to the survey area to limit ferry time and fuel consumption.

## 3.0 Property Geology

The Ida Oro prospect was discovered during a regional followup by silt sampling of areas anomalous in mercury detected during an earlier Geological Survey of Canada silt sampling program. Disseminated gold occurs within a 2 by 1.8 km area of bleached and silicified rocks of the Ordovician to Lower Devonian aged Road River Group, which includes calcareous grey shale and siltstone, grey chert and siliceous shale and black graphitic shale. The sedimentary rocks which been intruded by a number of small stocks, dykes and plugs of Cretaceous aged hornblende monzonite, have been hydrothermally altered adjacent to the intrusive bodies as evidenced by argillic and silicic alteration of the sediments. (from Minfile report 116A027)

## 4.0 Survey Procedures & Personnel

The survey was flown according to the specifications outlined in Table One. The survey lines (as flown) were trimmed within a Geosoft database to the survey polygon plus 100m. This resulted in the number of l-km as described in Table One.

Nominal bird height was 60 m. In some cases the bird height was higher, especially in areas where the cliffs made it difficult to climb and descend quickly. Over flatter areas, the bird height was closer to 40 m.

Nominal survey speed was approximately 100 km/hr. Sampling of all data, including GPS, occurred at a 10 Hz rate. Therefore the approximate lateral distance between readings was 2.5-3.0 m.

Real-time helicopter navigation was possible using the AgNav system. GPS sensor positioning was provided using a Novatel 10-channel receiver set to the CD-GPS mode (western zone). This mode is considered the most accurate in Canada and provides real-time accuracy of ~ 1-5 m. The GPS antenna was installed on top of the gradiometer bird, near the center (length-wise) of the housing.

A radar altimeter was connected to the skid gear of the helicopter and provided a measurement of distance above ground for the pilot to navigate by. Inside the helicopter the radar altimeter had a digital readout attached to the dash board.

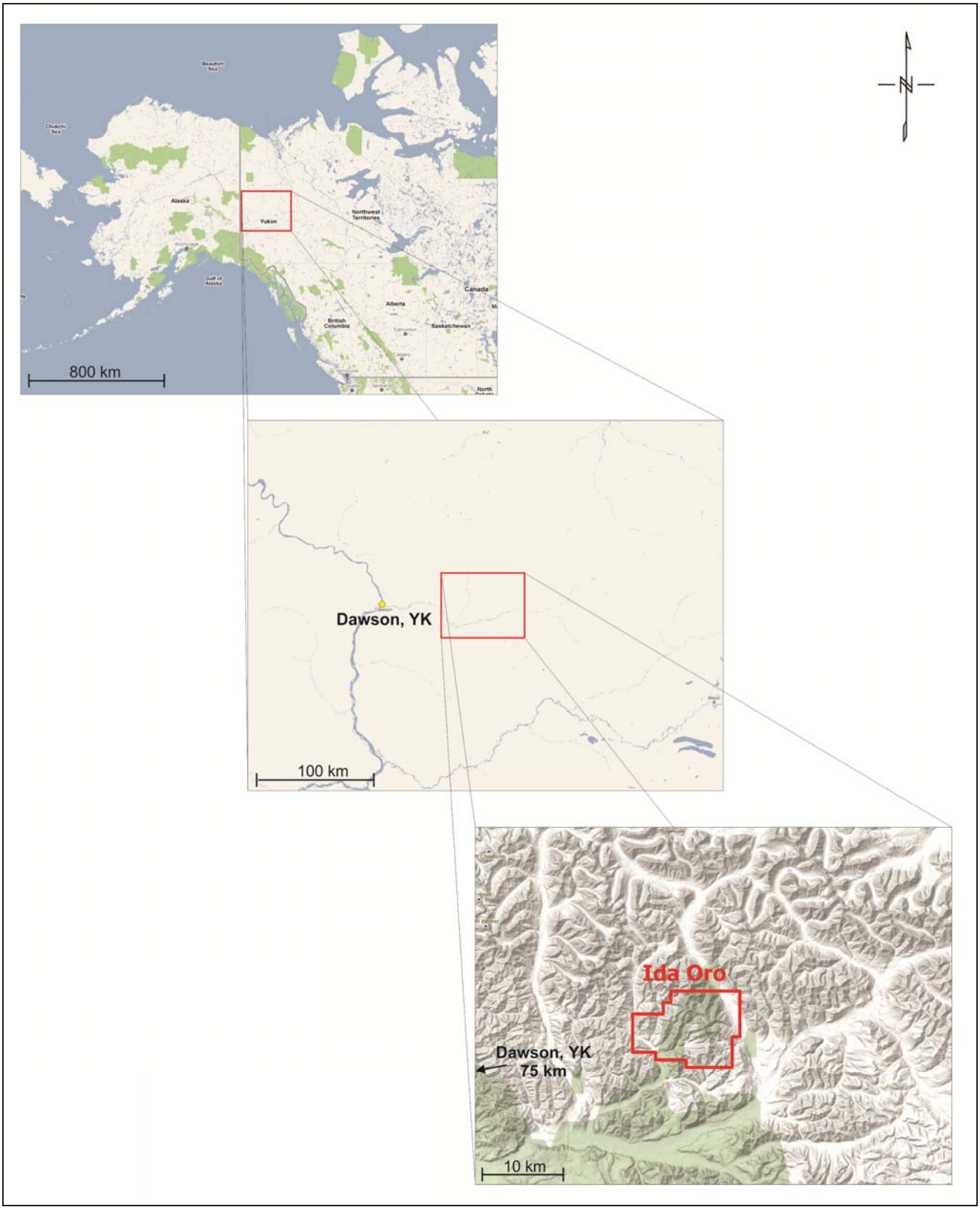


**Figure 1 - Regional location of the Ida Oro survey area.**

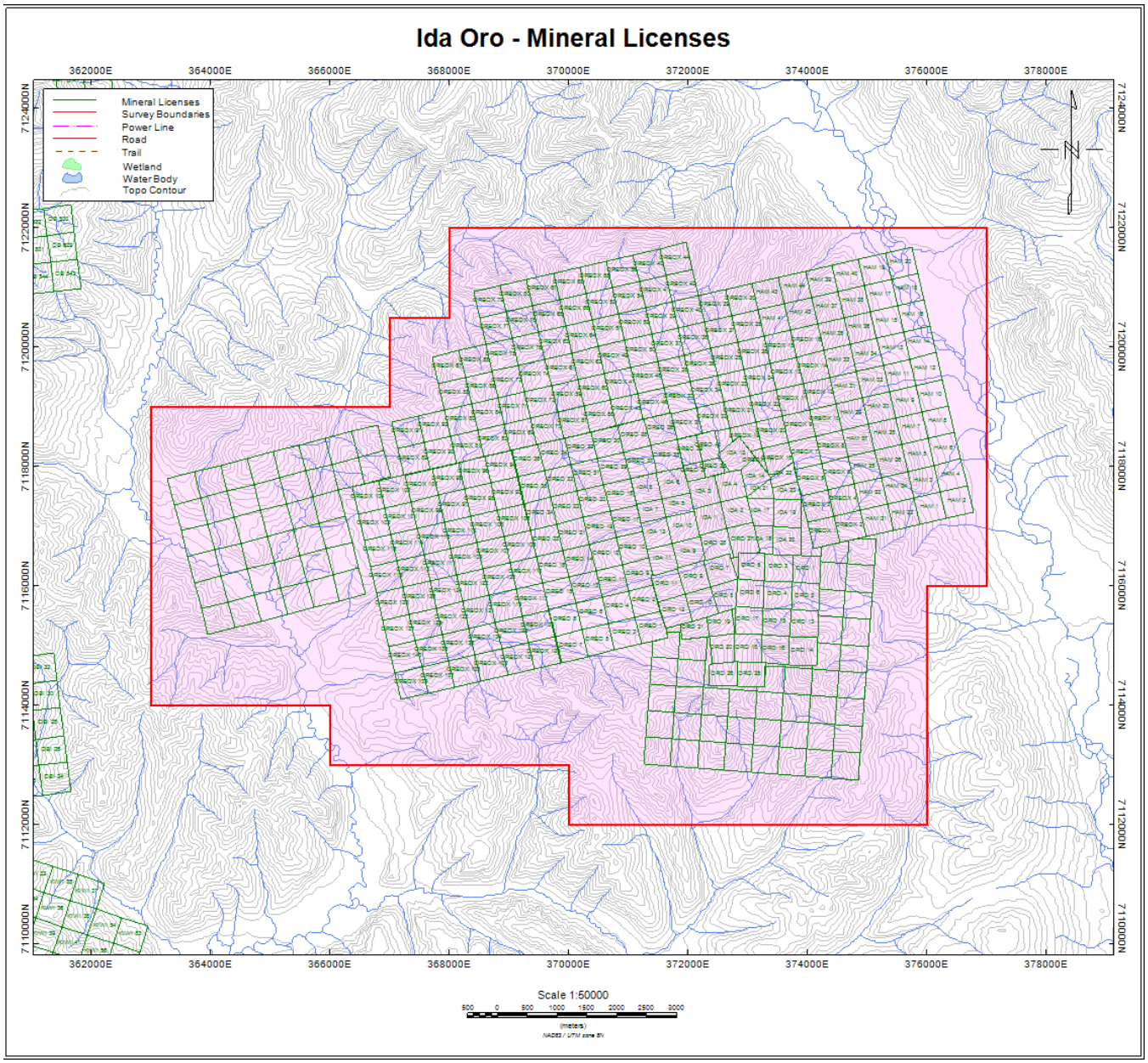


**Figure 2 – Ida Oro property with topographic contours and mineral claims.**

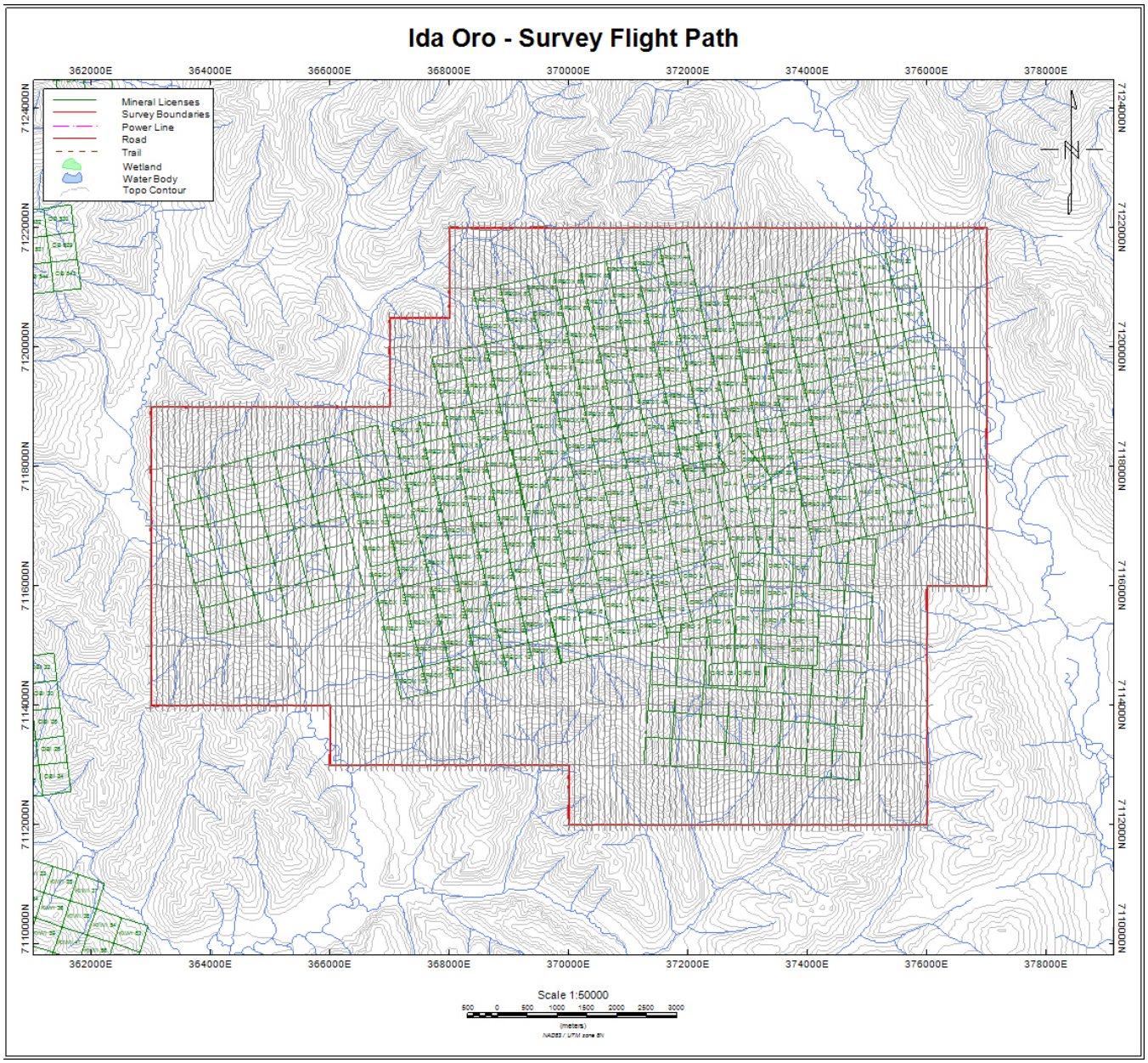


**Figure 3 - Flight path & survey outline of the Ida Oro survey area.**

Approximately one hour before the survey began, the base station magnetometer initialized and a VLF sensor attached. All transmitting VLF stations were scanned and the two stations with the strongest signals selected. The selected stations were then relayed to the operator who set them in the helicopter data system for recording during flight. The base station was turned off after the crew landed and contacted the processor.

(Table 1 provides a listing of all personnel involved in the project, their respective positions and a brief description of their roles and responsibilities throughout the survey.

Final data processing was carried out under the supervision of Sean Scrivens P.Geo., the Manager of Processing & Interpretation of Canadian Mining Geophysics Ltd.

**Table 1 - List of Survey Personnel**

| Individual | Position | Description |
|---|---|---|
| Rick Klassen | Pilot | Flew the helicopter. |
| Rob Whittmack<br>Lee Cooke | Aircraft Mechanic | Ensure helicopter maintenance is performed. |
| Dan LeBlanc | Operator | In-flight quality control & maintenance of the system and ancillary equipment. |
| Sean Scrivens | Processor | Off-site data processing. |
| Sean Scrivens | Final Processing & Reporting | Integration of field data into Geosoft database and generation of grids, profiles, map products and logistics report write-up. |
| Sean Scrivens | Interpretation | Final review of data interpretation write-up and recommendations |
| David Schmidt | Client Representative | President & CEO of Ryan Gold Inc. |

**Table 2 - Survey Area Specifications**

| Area | Line Direction | Line Spacing | Number of km |
|---|---|---|---|
| Ida Oro | N0°E | 100 m lines | 1,170.3 km |
| | N90°E | 1000 m lines | 128.8 km |

# 5.0 Equipment

## 5.1 The Helicopter

The helicopter used was a Eurocopter AStar Aerospatial 350 B2 with registration C-GPWO, owned and operated by Vancouver Island Helicopters (VIH). An AStar B2 is shown in Figure 4.

Installation of the ancillary equipment was performed at VIH's hangar in Prince George, BC. Two short test flights were performed to ensure the system was operational. The bird was then towed to the Princeton, BC region where surveying commenced immediately.

The gradiometer system was attached to the helicopter by a 30 m long tow cable. The tow cable contains a Kevlar strength member and a weak link. The tow cable also contains the power and signal wires.


**Figure 4 - The survey used an AStar B2 similar to the above.**

## 5.2 The Gradiometer

The CMG magnetic gradiometer (Figure 5) is based on GEM System potassium magnetometers. These sensors are preferred over the cesium optically pumped sensors because they have a lower effective noise level (better for gradient measurements) and a much lower heading error (less absolute correction required from line to line).

Three sensors are also preferred over the normal four sensor arrays featured on systems that measure all three magnetic gradients. CMG measures the vertical gradient from the top sensor and the average of the two bottom sensors located 2.95 m apart and the cross-line (or transverse) gradient from the two side sensors located 3.45 m apart. The in-line gradient is actually calculated from successive measurements of the average of the two side sensors given the fact that measurements along the flight line are acquired at approximately the same distance as the sensor separation of the bird.

Computing the in-line gradient as opposed to measuring it directly using an additional sensor has some important advantages. Firstly, and most importantly, by having only three magnetometer sensors, they can all be placed at the front of the bird and the magnetically noisy electronics (including the tow cable) can all be placed at the back of the bird so that the distance between sensors and electronics is maximized. Secondly, the computed in-line measurement has effectively no heading error (the readings are measured from the same sensors and are constant across such a short distance), and is relatively free from diurnal variations in the magnetic field, given the short time interval (0.1 sec) between readings.

**Figure 5 - The CMG tri-axial magnetic gradiometer.**

**Table 3 - Specifications for the CMG Magnetometer Section**

| | |
|---|---|
| Sensitivity: | +/- 0.001 nT |
| Absolute accuracy: | +/- 0.5 nT over operating range maximum |
| Sample rate: | 10 Hz (0.1 sec) |

| | |
|---|---|
| Dynamic range: | 30,000 to 90,000 nT, 5,000 nT/m gradient |
| Heading error: | +/-0.15 nT maximum for all sensor orientations |
| Operating temperature: | -32° C to +40° C normally |
| Tuning method: | Dynamic re-starting at 30,000 nT |
| Volume of sensor: | 70 $mm^3$ |

The magnetometer data is collected at a rate of 10 Hz. The frequency from each sensor is counted separately within the digital electronic section located approximately 4.5 m away from the sensors in the middle of the bird. The combined data stream (including mag, gps, vlf and radar information) is then sent up the tow cable to the data acquisition system in the helicopter. Specifications for the magnetometer sensors are given in Table 3.

### 5.3 The Magnetometer Bird

The magnetometer frame is constructed from fiberglass and the sensor housings are made from Kevlar. The horizontal displacement between magnetometer sensors is 3.45 m. The vertical separation is 2.95 m. The length of the bird is 5.3 m and weighs approximately 180 kg. The bird can be separated into two sections and the magnetometer arms removed for easy transportation.

### 5.4 The Spectrometer

The revolutionary RSX-5 digital airborne gamma-ray spectrometer (Figure 6) is designed for the detection and measurement of low-level radiation from both naturally occurring and man-made sources. The spectrometer was built by and purchased from Radiation Solutions Inc. The RSX-5 is a fully integrated system that includes an individual Advanced Digital Spectrometer (ADS) for each crystal within the box. The ADS records high resolution, 1024 channel, digital data of naturally occurring radioactive elements.

Key Features:

- 1024 channel resolution
- Individual crystal ADC and processing
- No distortion as each crystal output is fully linearized permitting multi-crystal summing without distortion
- Effectively no signal degradation
- No radioactive test sources required for system setup or system performance validation
- Extremely wide dynamic range
- High level of self-diagnostics
- Worldwide usability, fully multi-peak automatic gain stabilization on natural isotopes
- Data compression - individual crystal spectral data storage can be achieved with no effective increase in data volume


**Figure 6 - Radiation Solutions RSX-5 Gamma Ray Spectrometer.**

The recorded spectrometer data was transferred directly into the acquisition computer via high speed USB. The data was processed independently and merged with the magnetic data using GPS time stamp.

## 5.5 The VLF-EM System

The CMG gradiometer contains two VLF (very low frequency) EM receivers that can be tuned to any of the operational VLF transmitters worldwide. In general, two orthogonal stations are chosen such as Cutler Maine (24.0 kHz) and Jim Creek Seattle (24.8 kHz).

Measurements of the in-phase, quadrature-phase and total field are taken at a 10 Hz sample rate. The in-phase measurement is easily affected by variations in the sensor orientation and may not be useful in areas of rugged topography or where bird movement is significant. The quadrature-phase measurements are dependent on bird direction so alternating lines are sign inverted. The results can be gridded and provide the locations of weak conductors, given the high relative frequency of the transmitter station.

The measured VLF components are converted into a digital signal and then appended to the data string in the main magnetometer console. This entire data string is then transmitted up the tow cable to the data acquisition system in the helicopter.

### 5.6 The Magnetometer Base Station

A GSM-19 base station was used to record variations in the earth's magnetic field and referenced into the master database using GPS time stamp. This system is based on the Overhauser principle and records total magnetic field to within +/- 0.02 nT at a one (1) second time interval.

The GSM-19 is portable and can be placed in a remote location without the need for extra batteries or cabling. On this survey the unit was positioned at a magnetically quiet location at the mine site.

### 5.7 The Radar Altimeter

The CMG system uses two radar altimeters, both modulated frequency radio versions manufactured by Free Flight. The radar altimeter in the helicopter is used by the pilot to estimate terrain. The second altimeter, mounted directly on the bird, provides an accurate measurement of bird height. The approximate accuracy of these devices is +/- 2 m.

### 5.8 GPS Navigation

CMG uses the AgNav Incorporated (AgNav-2 version) GPS navigation system for real-time locating while surveying. The AgNav unit is connected to a Tee-Jet GPS system receiver that uses the WAAS system – considered to be a standard in aircraft navigation and accurate throughout a large portion of Canada.

### 5.9 Data Acquisition System

Data is collected by the main magnetometer console in the gradiometer bird and includes GPS timing and positional information, magnetometer readings, VLF readings, and radar altimeter. This information is digitized inside the console, all at a rate of 10 Hz. The resulting data string is transmitted in digital format along the tow cable into a laptop computer inside the helicopter that is running the GEM Systems DAS software. All data is stored on the hard-drive in ASCII format using a simple column by row format.

## 6.0 Deliverables

From the survey, a number of deliverable products are generated including a set of hard-copy maps, a final report (this document), and a digital archive of the data with digital copies of map products.

### 6.1 Hardcopy Products

Hardcopy map products are provided at 1:20,000 scale and include a topographic back-drop. Each map contains a scale bar, north arrow, coordinate outlines (easting & northing), flight lines with line number and direction and geophysical data.

The survey block consisted of 1 map plate customized to fit within the boundaries of a 42" plotter. Each map contains a technical summary of specifications and a colour bar that describes the geophysical data.

### 6.2 Digital Products

The geophysical data is provided in a Geosoft GDB database. At the Client's request an xyz archive of the same database in ASCII format can also be provided.

The contents of the database are described more fully in Appendix B. A copy of the GDB database is kept by CMG as a courtesy to the Client but can be deleted at the Client's request.

In addition to the GDB file database, copies of all geophysical grids are provided as GRD files (also in Geosoft format). The cell size used for gridding is nominally 1/5 of the flight line spacing.

Map files in Geosoft MAP format are also provided as deliverables. The Client can use a free viewer available from Geosoft Limited (www.geosoft.com) for viewing and plotting map files, but not for editing or changing them.

### 6.3 Delivered Products

The following map products were delivered in hard-copy and digital (Geosoft Map & PDF) format. Each map product was colour shaded on a topographic backdrop with flight lines and contours.

- Total magnetic field reduced to poles (TMI-RTP)
- Magnetic Analytical signal (ASIG)
- Measured in-line horizontal field derivative (MI-HMG)
- Radiometrics corrected total count (GRS-TC)
- Radiometrics Thorium-Potassium ratio (GRS_Th-K)

The following map products were delivered in digital (Geosoft Map & PDF) format only (in addition to those above). Each map product was colour shaded on a topographic backdrop with flight lines and contours.

- Total magnetic field (TMI)
- Measured cross-line horizontal magnetic field derivative (MC-HMG)
- Measured in-line horizontal magnetic field derivative (MI-HMG)

- Radiometrics percent Potassium (GRS-K)
- Radiometrics equivalent Uranium (GRS-U)
- Radiometrics equivalent Thorium (GRS-Th)
- Radiometrics Uranium-Potassium ratio (GRS_U-K)
- Radiometrics Uranium-Thorium ratio (GRS_U-Th)
- Radiometrics Ternary image
- Magnetic 1st vertical Derivative (1VD)
- Magnetic 2nd vertical Derivative (2VD)

The following grid products were delivered in digital (Geosoft GRD) format only (in addition to those above).

- Digital Terrain Model (DTM)

The following additional products were delivered in digital format:

- Copy of this report in .pdf format
- Geosoft database GDB of all collected data
- Geosoft and Acrobat software utilities for data viewing

## 7.0 Processing

Preliminary data processing is performed using CMG proprietary methods. This includes calculation of the magnetic gradients from the three sensors (MAG1, MAG2 and MAG3), digital terrain model, bird height, and merging of the base station magnetic data (sampled at 1.0 sec) with the survey data (sampled at 0.1 sec).

### 7.1 Base Maps

All base maps are presented in the Datum and Projection defined in the Introduction of this report. All map coordinates refer to projected easting and northing in meters. All maps contain the actual flight paths as recorded during surveying and have been clipped to the survey polygon with a 100m extension.

The topographic vector data has been obtained from Natural Resources Canada.

Topographic shading has been derived from 90 m resolution digital elevation model (DEM) data provided by the NASA Shuttle Radar Topography Mission (SRTM) and shaded at an inclination and declination of 45º.

### 7.2 Flight Path

The helicopter used "ideal" flight lines as guidance during surveying as displayed on the real-time AgNav system with the aid of a helicopter mounted GPS. A separate GPS mounted to the bird was used to record actual position. The sample rate of the GPS was 10 Hz, the same as all the other data collected in flight.

The GPS outputted both latitude and longitude values and easting and northing values, all in the WGS84 Datum, using the UTM Projection Zone 8 North. There has been no interpolation of the positional data, nor has there been any filtering of the data.

### 7.3 Terrain Clearance

Two radar altimeters recorded data during the course of the survey: one located on the skid gear of the helicopter and the other on the base of the bird. The helicopter mounted radar altimeter was used to maintain terrain clearance by the pilot. A digital indicator was mounted on the dashboard of the helicopter. This work was performed by a licensed helicopter engineer provided by VIH.

The digital terrain model (DTM) was derived by subtracting the bird mounted radar altimeter value from the GPS z position (mean point above sea level). The DTM values were further corrected for a lag value of 1.0 sec. The DTM values are to be considered relative as they have not been tied into any surveyed geodetic point.

### 7.4 Magnetic Data Processing

The magnetic data were collected without any lag time, therefore a lag time correction was not applied. In areas where one magnetometer sensor has become unlocked, the total magnetic field values for that sensor were replaced with a dummy value ("*"). The lock and heater settings are both used for QC measures so it is easy to find the areas where one or more sensors lost lock or were not heating correctly. Locking errors occur almost entirely on turn-arounds.

The raw ASCII survey data files and basemag ASCII data files are imported into separate Geosoft databases. A QC check of the basemag data is made on a day to day basis, exported as a Geosoft Table file (TBL) and merged with the active database using built-in Geosoft routines.

Diurnal magnetic corrections were applied only to the channel that was used to generate a total magnetic field map. The MAG1, MAG2, and MAG3 sensor values were used to generate the gradients and do not require diurnal correction. The base station data was linearly interpolated from a 1.0 sec sample rate to 0.1 sec to correspond to the flight data.

The horizontal gradients are sensitive to line direction. Positive polarity is defined as to the north and east. On south- and/or west-facing lines the horizontal gradients are multiplied by -1.

The magnetic data from the individual sensors as well as the computed total magnetic intensity have no filtering applied. The computed gradients are lightly filtered to remove high frequency noise common in areas of rough terrain or flying conditions. The magnetic data grids were tie line-leveled if needed and the resulting grids micro-leveled.

### 7.4.1 Magnetic Analytic Signal

The magnetic analytic signal (ASIG) is calculated by taking the square root of the sum of the squares of each of the 3 axis components of the gridding total magnetic intensity data. The equation for the analytic signal is:

$$\mathrm{ASIG} = \sqrt{\left[\left(\frac{\mathrm{dT}}{\mathrm{dx}}\right)^2 + \left(\frac{\mathrm{dT}}{\mathrm{dy}}\right)^2 + \left(\frac{\mathrm{dT}}{\mathrm{dz}}\right)^2\right]}$$

where dT/dx is the in-line gradient, dT/dy is the cross-line gradient and dT/dz is the vertical gradient of the total magnetic field.

In general, the analytic signal is a gradient product that ignores the effects of target orientation. This "turns" all responses, regardless of how they interact with the earth's magnetic field, into the positive direction. Therefore, both negative anomalies & dipole effects will appear positive centered of the target source.

The analytic signal can be used to map the edge of large magnetic bodies as well as bring to light anomalous trends that can appear insignificant in a TMI grid. The nature of the algorithm also strips out effects of deep regional responses and focuses more on the near surface.

### 7.4.2 Magnetic Tilt Derivative

The magnetic tilt derivative (TDR) combines all three gradients (X, Y and Z) to produce what is a called a tilt angle. This product highlights very subtle, near surface structures in the dataset where the zero contour line of the grid is said to represent geology contacts or edges of bodies.

The magnetic tilt derivative is calculated by the following equation:

$$\mathrm{TDR} = \tan^{-1}\left[\frac{{}^{\mathrm{dT}}/_{\mathrm{dz}}}{\sqrt{\left({}^{\mathrm{dT}}/_{\mathrm{dx}}{}^2 + {}^{\mathrm{dT}}/_{\mathrm{dy}}{}^2\right)}}\right]$$

where dT/dx is the in-line gradient, dT/dy is the cross-line gradient and dT/dz is the vertical gradient of the total magnetic field.

### 7.4.3 Magnetic Reduction to Poles

The shape of the magnetic response over a ferrous body is determined by the inclination and declination of the Earth's magnetic field at that location. The reduction to pole (RTP) process rotates the magnetic field response as if it were measured at the magnetic pole. The resulting response can then be viewed in map form with a vertical magnetic field inclination (90°) and a declination of zero (0°). By doing this, the interpretation of the data is less complex as vertical magnetic sources produce magnetic anomalies that are centered on the body symmetrically.

## 7.5 VLF-EM Data Processing

Due to the large distance to the nearest VLF station, the signal degradation was too high to produce any usable data throughout the survey. For this reason, no VLF products were produced. As the power output and functioning transmitting stations are out of CMG's control, VLF data is collected on an as is basis.

## 7.6 Radiometric Data Processing

The radiometrics data was processed using a variety of techniques used to strip out anomalous counts resulting from cosmic rays, aircraft and altitude. The data was stored on the RSX-5 spectrometer and imported directly into a separate Geosoft database. Here the data underwent a variety of corrections were applied, time lagged to match the magnetic data and exported to an ASCII XYZ. The file was converted in a table and merged with the master magnetic database. The radiometric data, collected a 1Hz, was merge using exact values and not interpolated to 10hz.

The cosmic background was identified by conducting a series of test flights at altitudes between 500m and 3000m at 500m increments. A linear regression of the cosmic window with each radioelement window produced an equation that accounted for aircraft background and cosmic scattering. These coefficients were stripped out of the data.

The stripping factors, unique for each spectrometer, were provided by Radiation Solutions and applied to the data. This correction removes the effects of Compton Scattering up and down the energy spectrum. The stripping coefficients were adjusted to compensate for aircraft altitude.

Height attenuation correction was applied to the data using a set of coefficient also supplied by Radio Solutioins. The radar altitude data was imported in the spectrometer database from the radar unit on the magnetometer and converted in standard temperature-pressure (STP). Attenuation coefficients were applied to each energy window as well as the total count.

Following all data corrections, each energy window was converted into their ground concentrations using supplied coefficients. This converts the potassium counts into %K, and the thorium and uranium counts into equivalent ground concentrations.

A set of radiometric ratios were also calculated using the final corrected data. These include a thorium-potassium ratio, a uranium-thorium ratio and a uranium-potassium ratio. All corrected data and ratios were included in the final database.

## 8.0 Results

The following images are shown in the corresponding figures. Each image has been color shaded with a sun angle of 45° inclination and 0° declination to enhance regions of high gradient. All grid products are processed independently and lightly micro leveled for the final product.

- The total magnetic field (TMI) is shown in Figure 7.
- The measured vertical magnetic gradient (M-VMG) is shown in Figure 8.
- The measured in-line horizontal magnetic gradient (MI-HMG) is shown in Figure 9.
- The measured cross-line horizontal magnetic gradient (MC-HMG) is shown in Figure 10.
- The calculated magnetic analytical signal (ASIG) is shown in Figure 11.
- The digital terrain model (DTM) is shown in Figure 12 with an elevation color transform.
- The Gamma Ray Spectrometer corrected total count is shown in Figure 13.
- The Gamma Ray Spectrometer percent Potassium is shown in Figure 14.
- The Gamma Ray Spectrometer equivalent Uranium is shown in Figure 15.
- The Gamma Ray Spectrometer equivalent Thorium is shown in Figure 16.
- The Gamma Ray Spectrometer Thorium – Potassium ratio is shown in Figure 17.
- The Gamma Ray Spectrometer Uranium – Potassium ratio is shown in Figure 18.
- The Gamma Ray Spectrometer Uranium – Thorium ratio is shown in Figure 19.
- The Gamma Ray Spectrometer Ternary is shown in Figure 20.
- The TMI Reduced to Poles (TMI-RTP) is shown in Figure 21.
- The TMI 1st Vertical Derivative is shown in Figure 22.
- The TMI 2nd Vertical Derivative Image is shown in Figure 23.

## 9.0 Interpretation

In the current survey, CMG has acquired high resolution magnetic gradiometer data and radioelement profiles. The vertical magnetic gradient provides a more accurate estimate of magnetic boundaries. The

cross-line horizontal gradient highlights structures that may be oriented sub-parallel to the flight direction. The vector sum of the three magnetic gradients – known as the analytic signal – produces highs directly over magnetic sources that are independent of the direction of the earth's magnetization vector.

### 9.1 Magnetics

The magnetic fabric of the area is complex and defines features that appear related to structures such as faults, veins, and/or fractures as well as clear intrusive outlines. The magnetic field responses vary considerably in both amplitude and character. For example, the broad and low gradient features likely represent deeper seated bodies, whereas the sharp and high gradient responses are related to near surface features. Based on the previous geological findings in the area, the primary targets of interest are thought to be magmatic bodies that have intruded into the Harlan group. These intrusions have the potential to host economic mineralization. Fractures and faults that intersect these intrusive bodies are primary areas of interest for hydrothermal deposition.

The individual magnetic products have been referenced in order to better define the numerous structures throughout the area. The various gradient and derivative products fully represent the components of the magnetic field and can provide specific information not obvious in the total field data. The in-line horizontal magnetic gradient (MI-HMG) emphasizes subtle magnetic features perpendicular to the line direction, whereas the first vertical derivative product (1VD) emphasizes all subtle features in the data. The magnetic analytic signal (ASIG) is produced by calculating the vector sum of all three magnetic gradients to produce a grid that is independent of the effect of orientation from subsurface bodies. Typically, the orientation of a magnetic target can produce a positive or negative response in the total magnetic field relative to its orientation.

The total magnetic intensity data (TMI) shown in Figure 7 illustrates the wide range of magnetic signatures within the Ida Oro survey area. The magnetic data ranges from 57,200 nT to 58,600 nT or approximately 1300 nT in peak to peak variation. The sharp responses, combined with a strong magnetic field response, indicate a shallow source. Based on the rough topography of the area, it is likely these features are exposed and are visible at the surface.

The majority of the localized magnetic peaks appear to occur within three intrusive bodies: 1 large and 2 smaller. These intrusion zones are clearly delineated in the magnetic analytic signal grid (Figure 24) as INT-01, INT-02 and INT-03. Outside of these intrusions, the regional geology exhibits several subtle structures which can be clearly seen in the 2VD grid product (Figure 25). The black lines represent ESE – WNW structures that appear to intersect the major intrusive bodies, however, whether they pre-date or post-date them is uncertain. The 2VD grid also shows two types of meandering features: localized highs depicted in green and localized lows depicted in purple. Upon closer examination, these features are following the topography of the area, where the highs are the mountain ridges and the lows are in the valleys (See Figure 26).

Further examination of the surrounding intrusions in the area, the two smaller bodies INT-02 and INT-03, appear to be single events without much variation in internal structure. However, INT-01 shows a complex array of structures increasing the likelihood of hydrothermal deposition (See Figure 27). Of additional interest within this intrusive body are two distinct magnetic lows, most visible in the ASIG data (Figure 28). These lows could represent demagnetized areas due to increased temperature

conditions or evidence of alteration. The radiometrics data has been referenced in supporting this conclusion.

### 9.2 Radiometrics

In addition to magnetics, a gamma ray spectrometry survey was performed to map the levels of radioactivity of the survey area. Individual spectrum gate data (Potassium, Uranium and Thorium) can provide valuable information on specific alteration or lithology types. The radiometric total count image shown in Figure 29 outlines several regions (dashed white line) with elevated radioactivity (sum of all spectrum gates). The majority of the radioactivity in the area appears to correlate quite well with the intrusive body INT-01 with some localized highs in the INT-02 and INT-03 intrusions.

Gridding the data as ratios of each radioactive element, such as "eTh vs pK" or "eU vs eTh", provides for a method of determining which areas may be relatively enriched or depleted in one of the radioelements. This could be the result of either primary causes (i.e. magmatic) or secondary causes (i.e. alteration related to magmatic, hydrothermal or weathering processes). In some cases, these processes are related to economic mineralization.

In particular, two regions are clearly visible as high eTh/K ratios, not only within the INT-01 body, but also within the magnetic low regions (See Figure 30). A high eTh/K ratio is an indicator of depleted potassium likely due to alteration. These areas should be ground truthed to determine the significance of this interpretation.

## 10.0 Conclusion

Based on the above discussion, a few areas are worth investigating further. In particular, the regional trending structures cross cutting the survey area may provide conduits for hydrothermal transportation of mineralization and should be closely examined in areas where they interest intrusions. INT-01 is the primary target of interest and requires additional study to identify any concentrations of mineralization within. The magnetic low areas, where they correlate with the high radiometric ratios (ROI-1 and ROI-2) are a good starting point for ground work. Grab samples or soil chemistry may shed light on the type of alteration at work and give clues as to the geologic system within this intrusive.

The surrounding intrusions, INT-02 and INT-03, are smaller in size but may be geologically similar to the main intrusion INT-01. These targets should be followed up should further exploration in INT-01 show promise of economic mineralization.

## 11.0 Recommendations

1. Conduct ground truthing and possibly geochemistry of the areas defined by ROI-01 and ROI-02 within the primary intrusive body, INT-01.

2. Perform investigation of the surrounding intrusions should the results from further work on INT-01 be favorable

3. Digital products from this report should be made available in either MapInfo or ArcView format as registered tiff files for integration into a GIS compilation.

4. Conduct an advanced level interpretation of the magnetic data, integrate with geology and possibly model selected structures.

Respectively Submitted,

Sean Scrivens P.Geo.
Canadian Mining Geophysics Ltd.
October, 2010

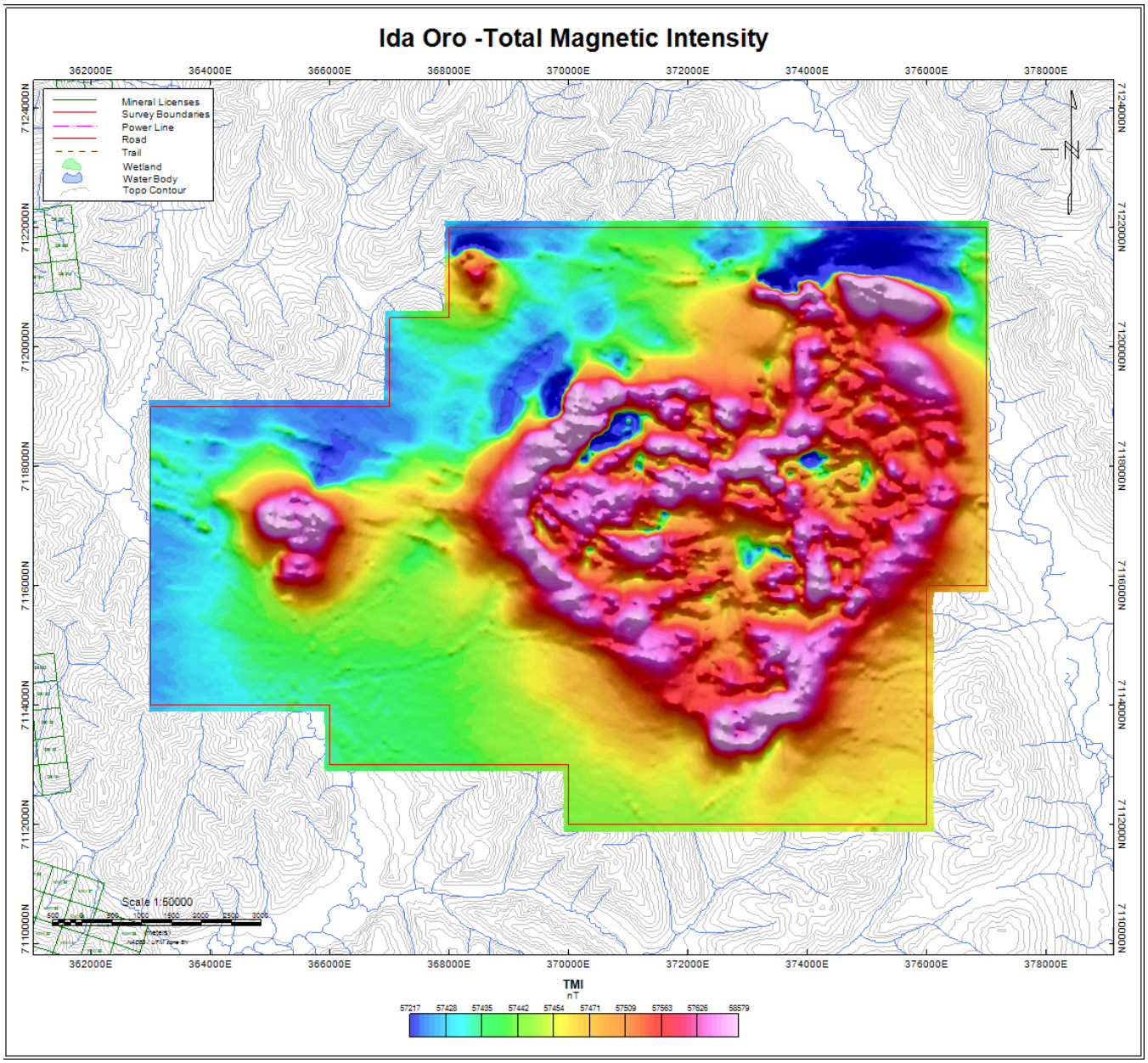


**Figure 7 - Shaded image of the total magnetic field intensity (TMI) over the Ida Oro survey area.**

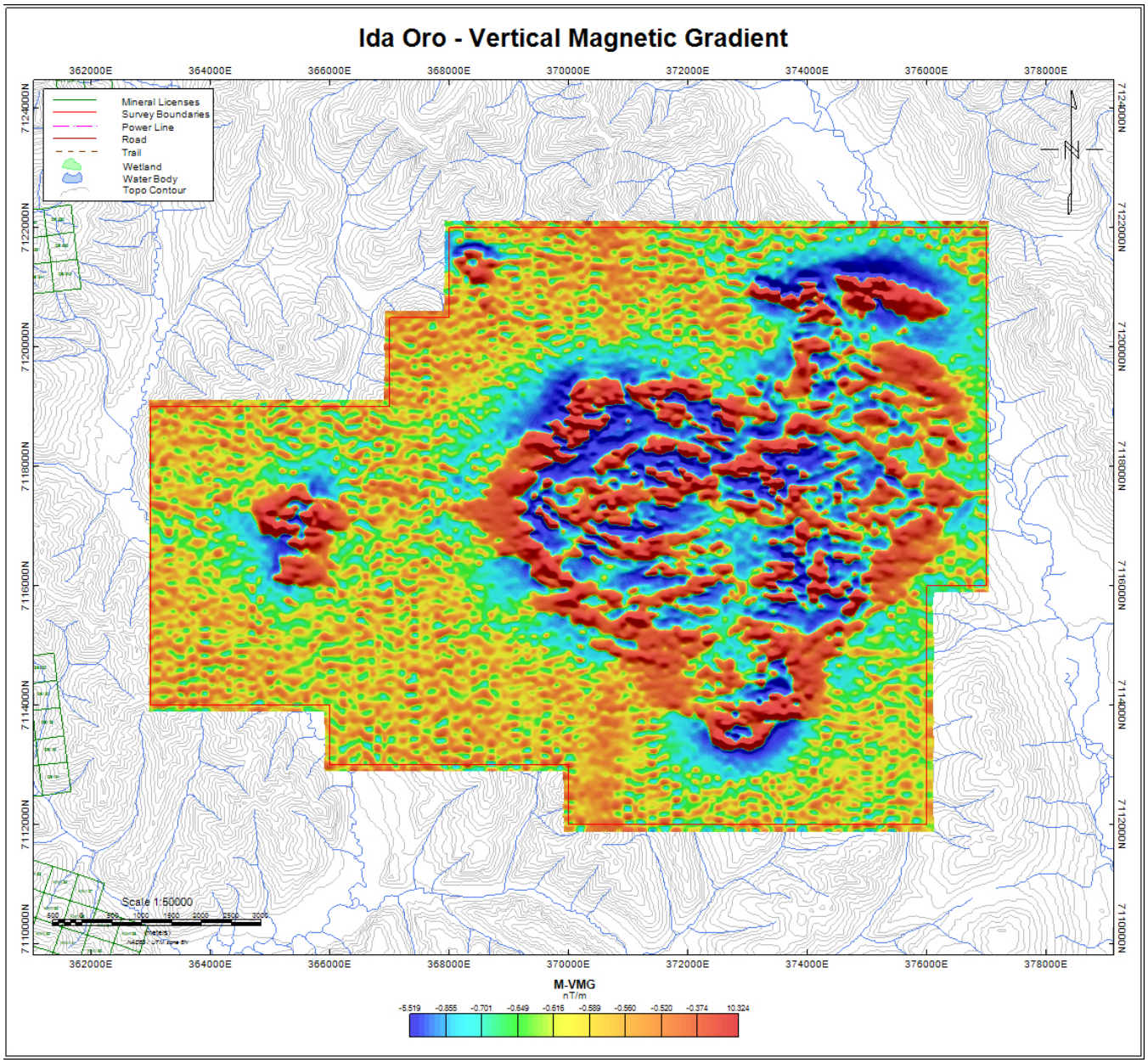


**Figure 8 - Shaded image of the vertical magnetic gradient (M-VMG) over the Ida Oro survey area.**

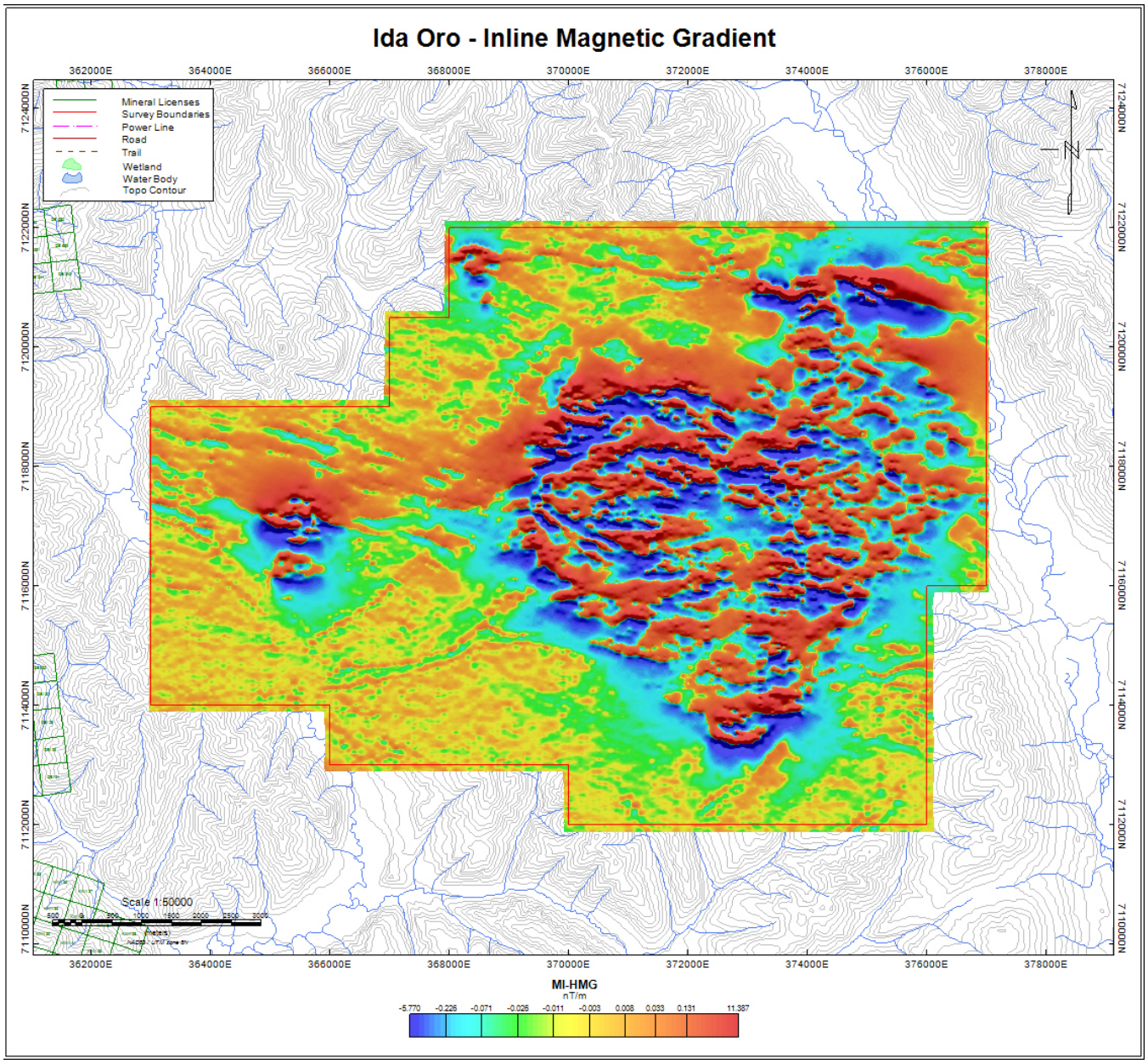


**Figure 9 - Shaded image of in-line horizontal magnetic (MI-HMG) over the Ida Oro survey area.**

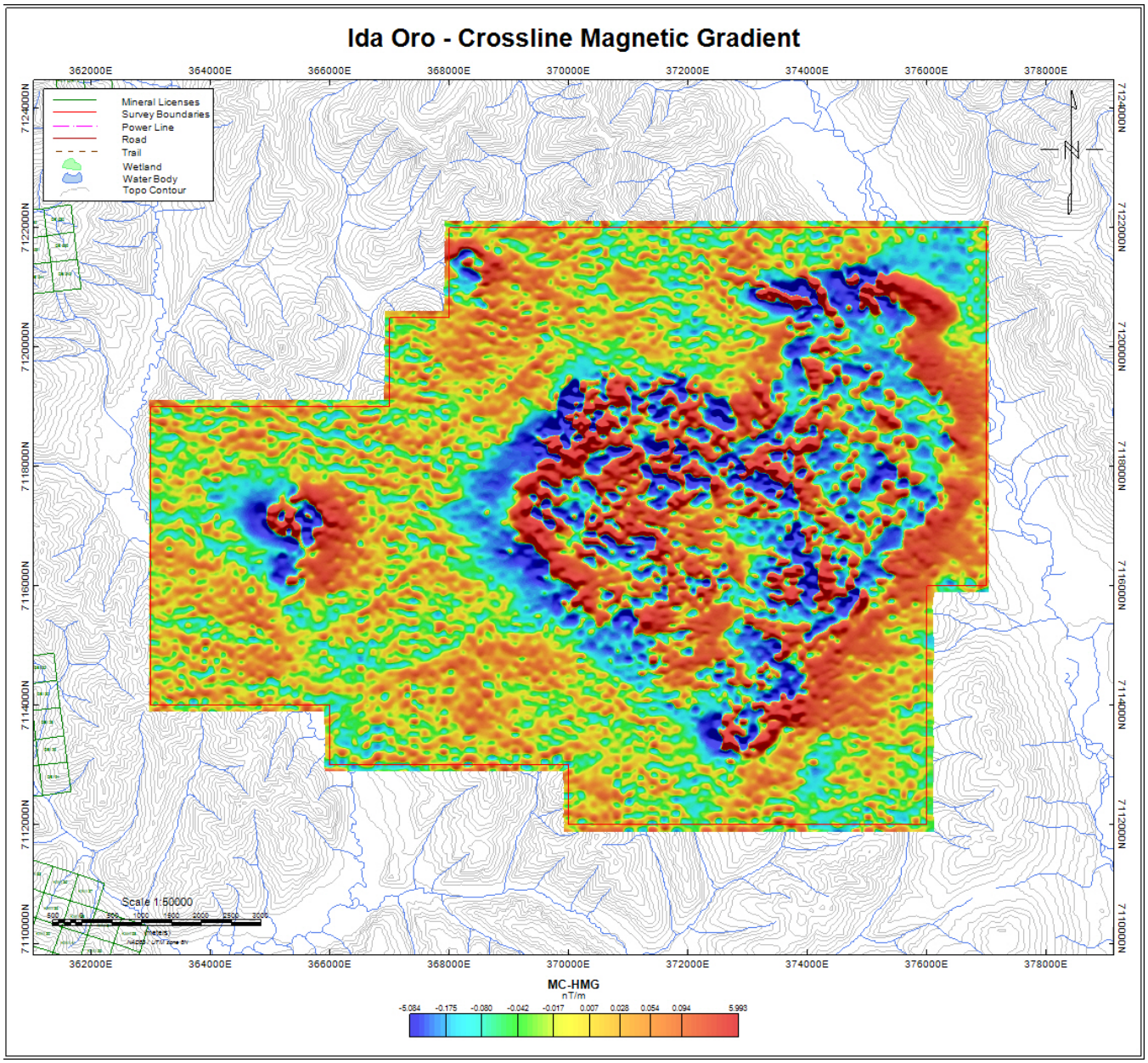


**Figure 10 - Shaded image of the cross-line gradient (MC-HMG) over the Ida Oro survey area.**

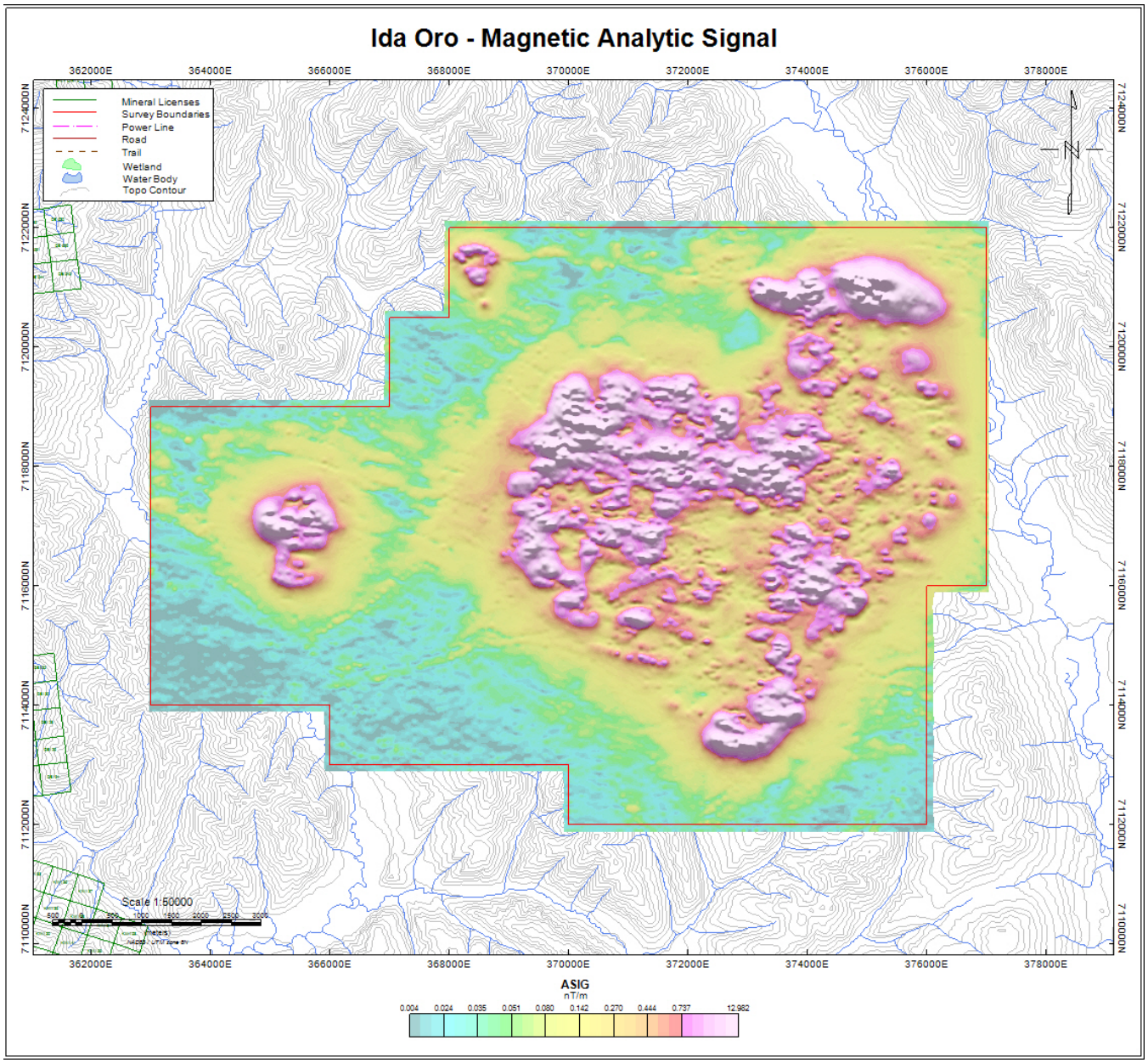


**Figure 11 - Shaded image of the magnetic analytical signal (ASIG) over the Ida Oro survey area.**

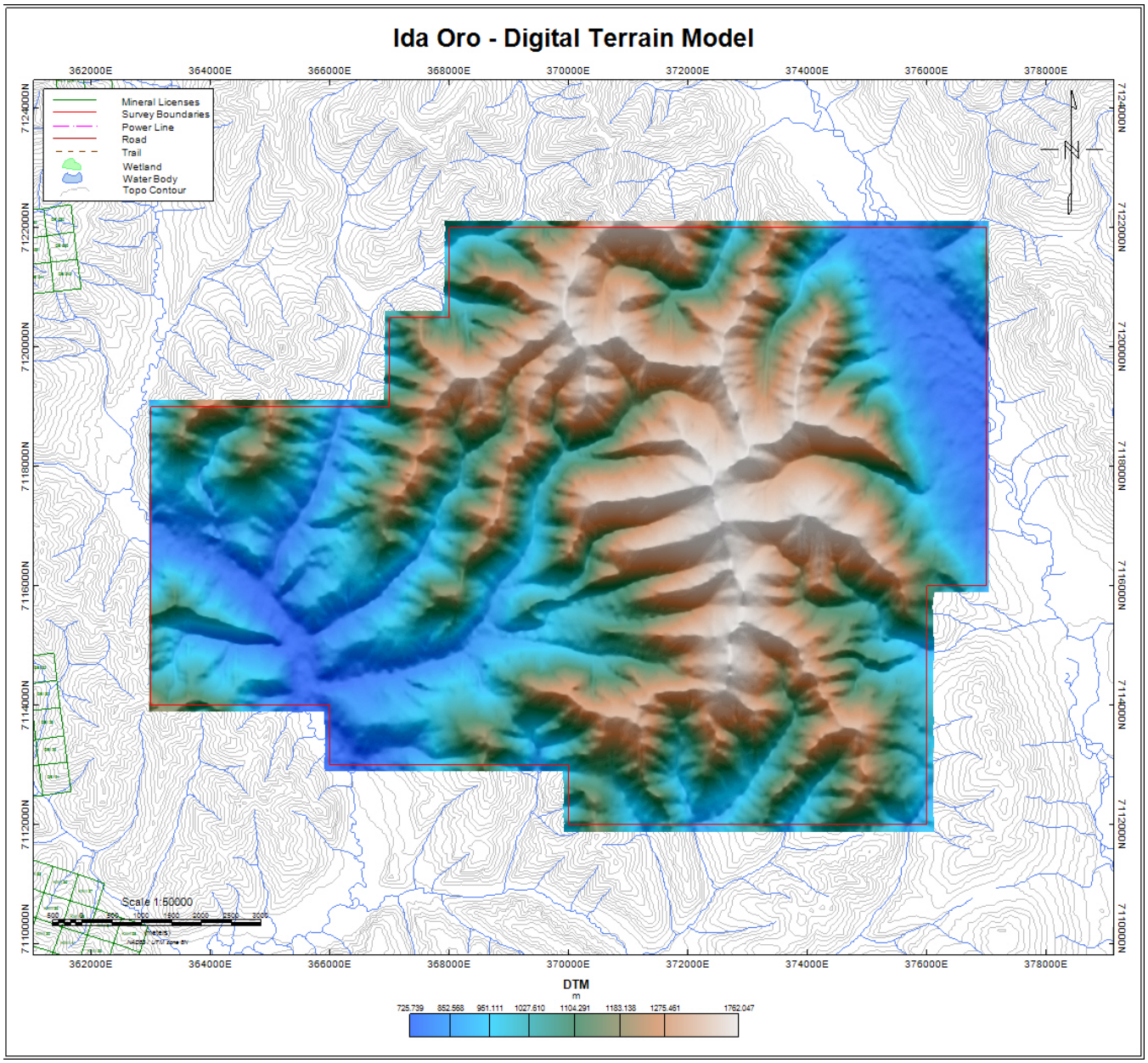


**Figure 12 - Shaded image of the digital terrain model (DTM) over the Ida Oro survey area.**

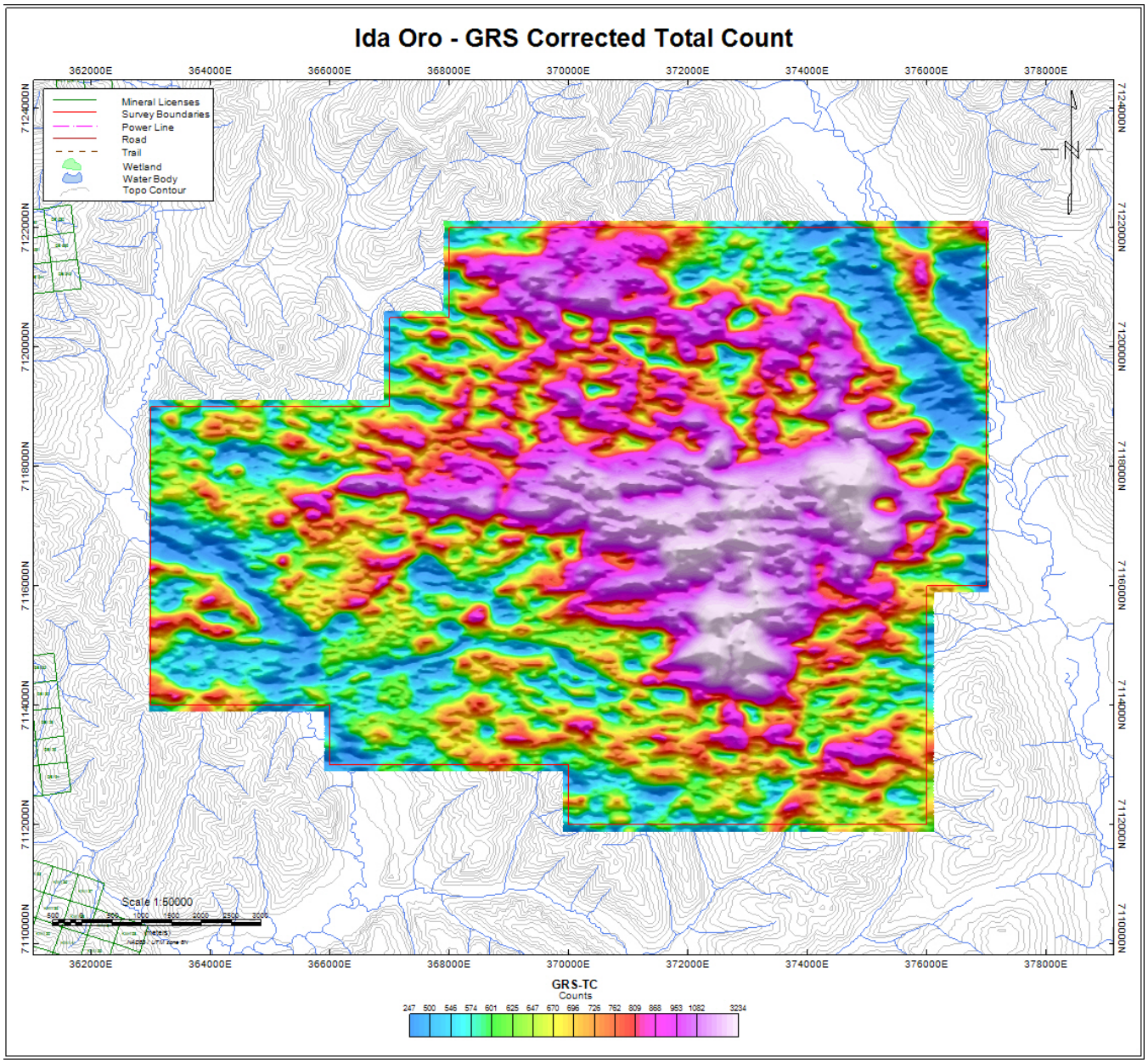


**Figure 13 - Shaded image of the radiometrics corrected total count over the Ida Oro survey area.**

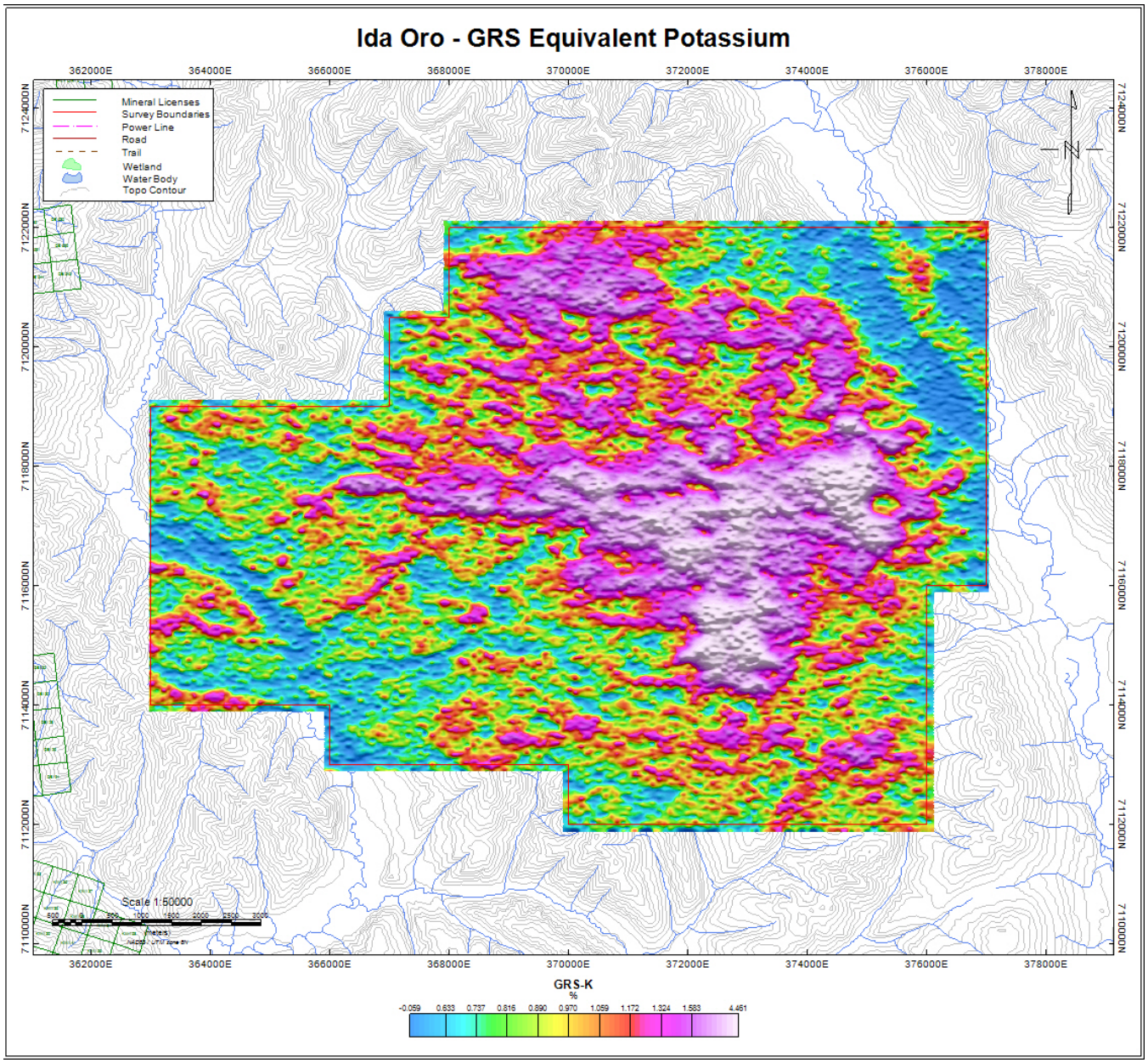


**Figure 14 - Shaded image of the radiometrics percent Potassium over the Ida Oro survey area.**

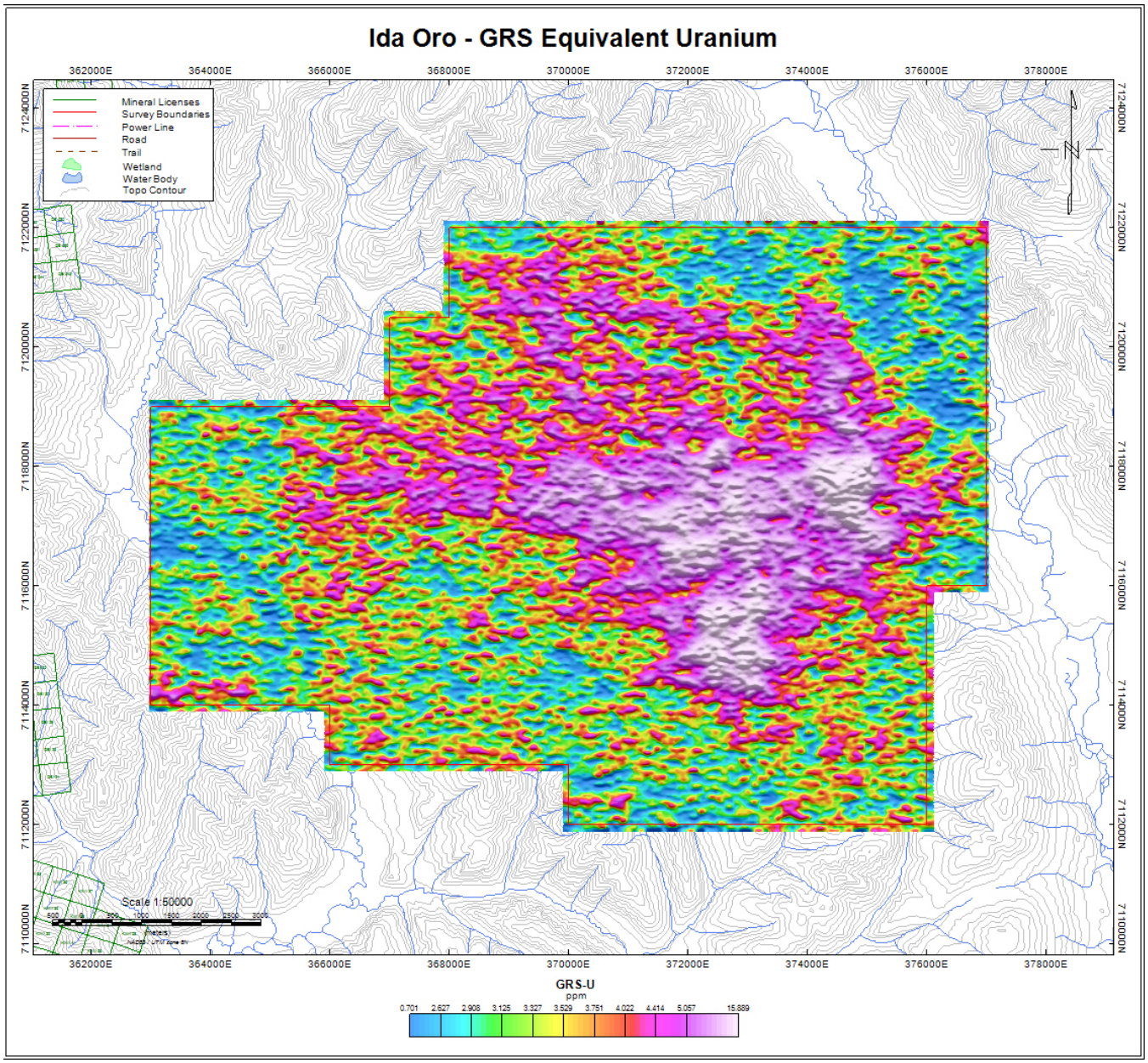


**Figure 15 - Shaded image of the radiometrics equivalent Uranium over the Ida Oro survey area.**

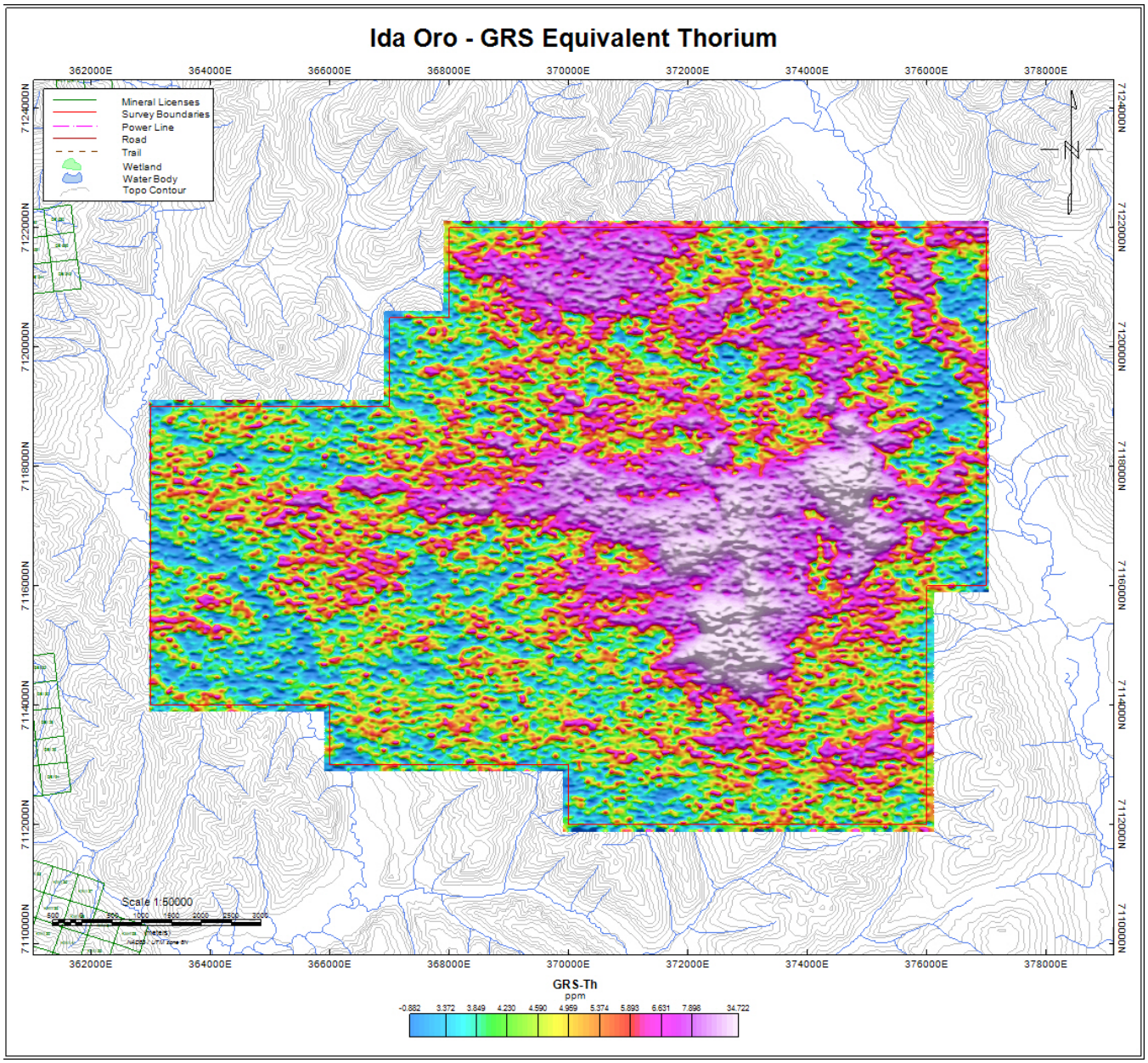


**Figure 16 - Shaded image of the radiometrics equivalent Thorium over the Ida Oro survey area.**

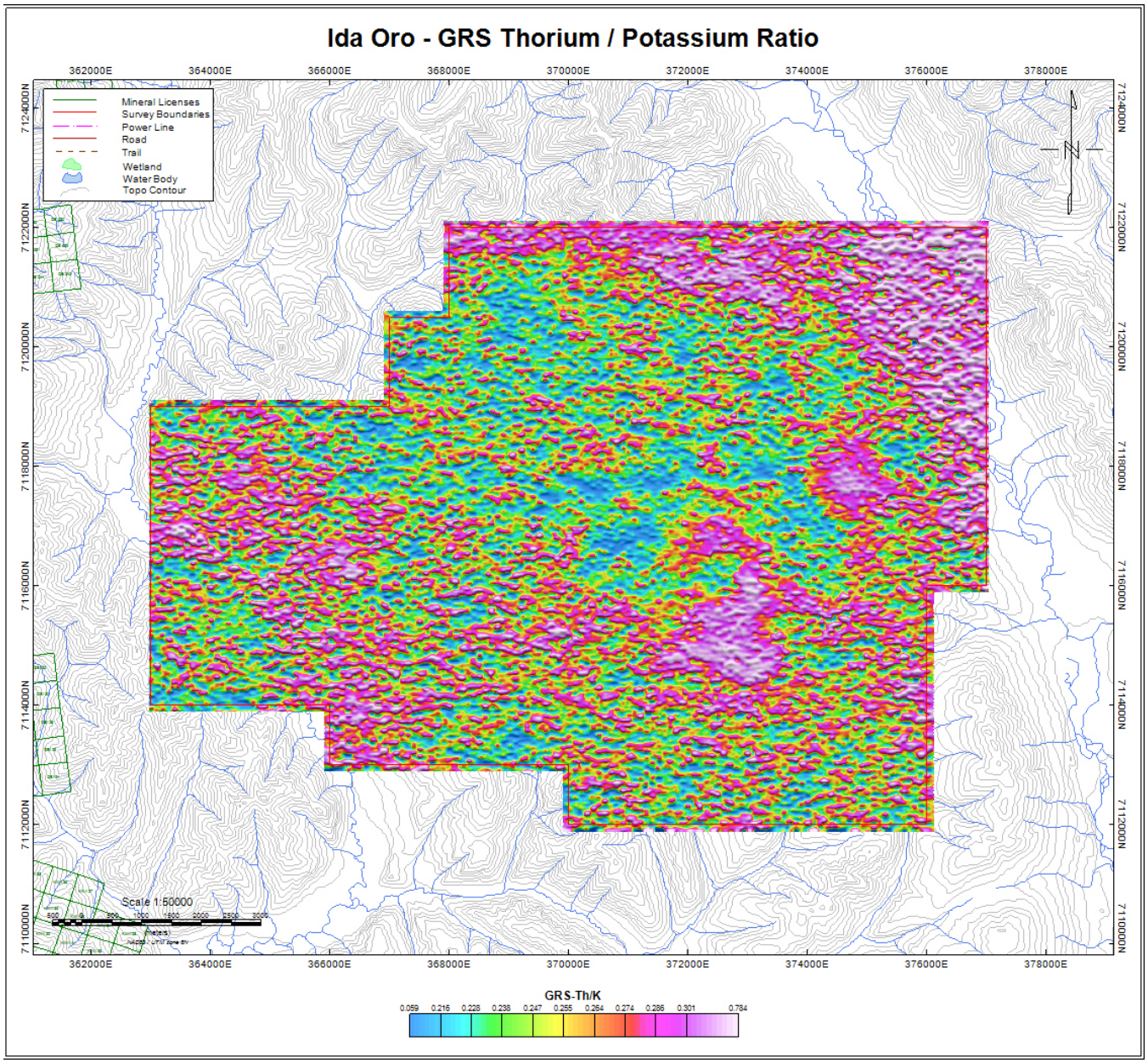


**Figure 17 – Shaded image of the radiometrics Thorium – Potassium ratio over the Ida Oro survey area.**

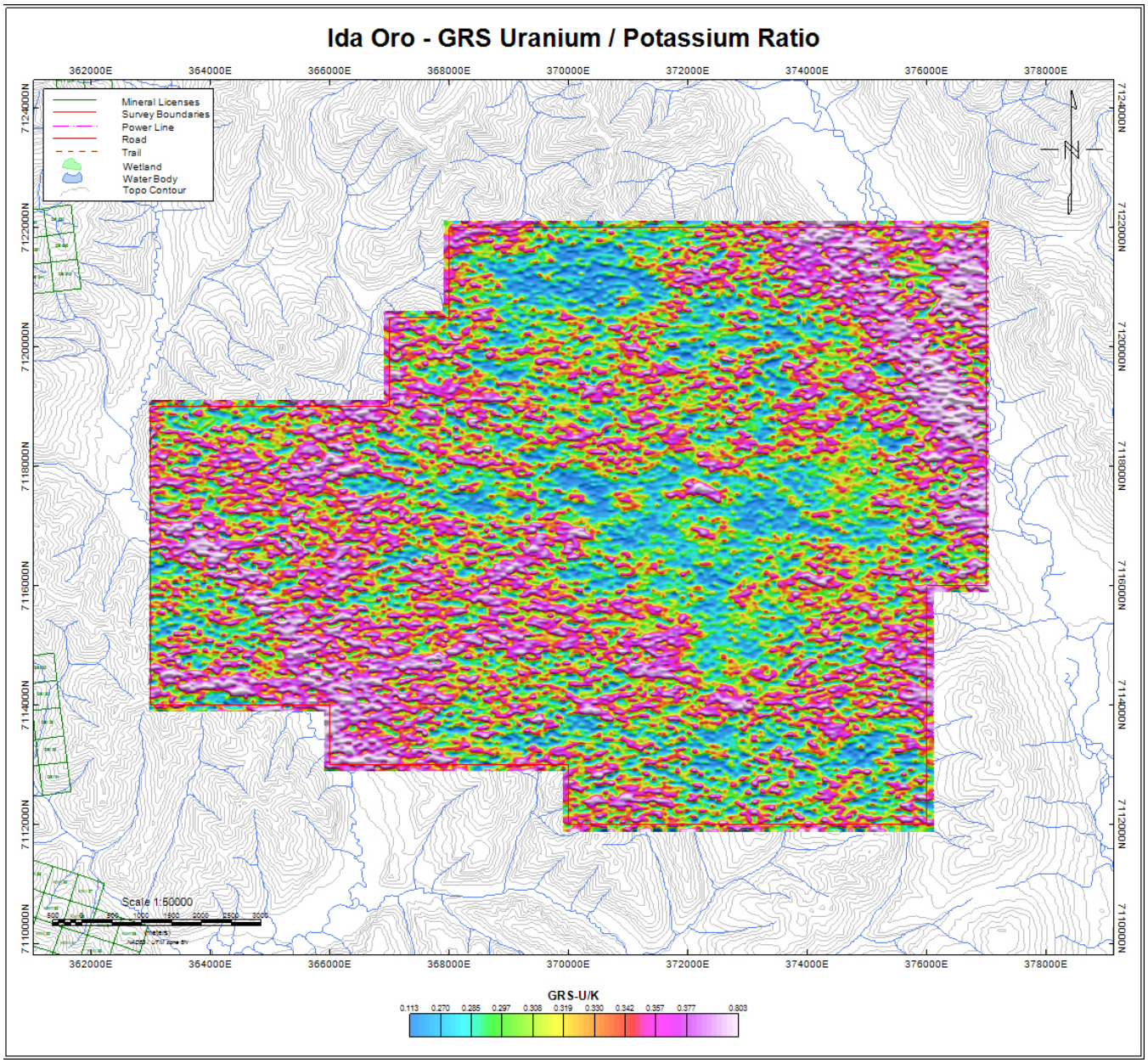


**Figure 18 – Shaded image of the radiometrics Uranium – Potassium ratio over the Ida Oro survey area.**

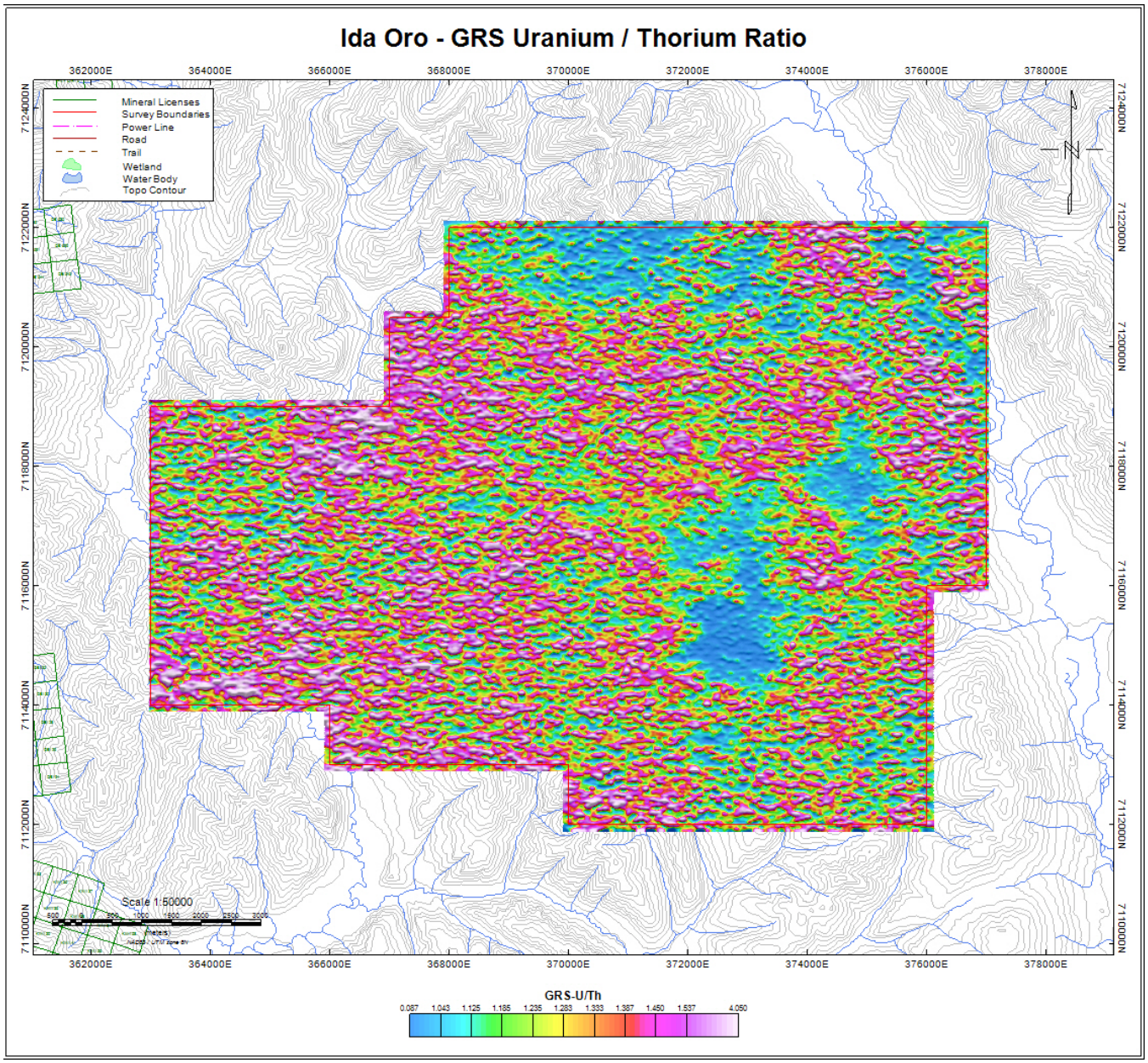


**Figure 19 – Shaded image of the radiometrics Uranium - Thorium ratio over the Ida Oro survey area.**

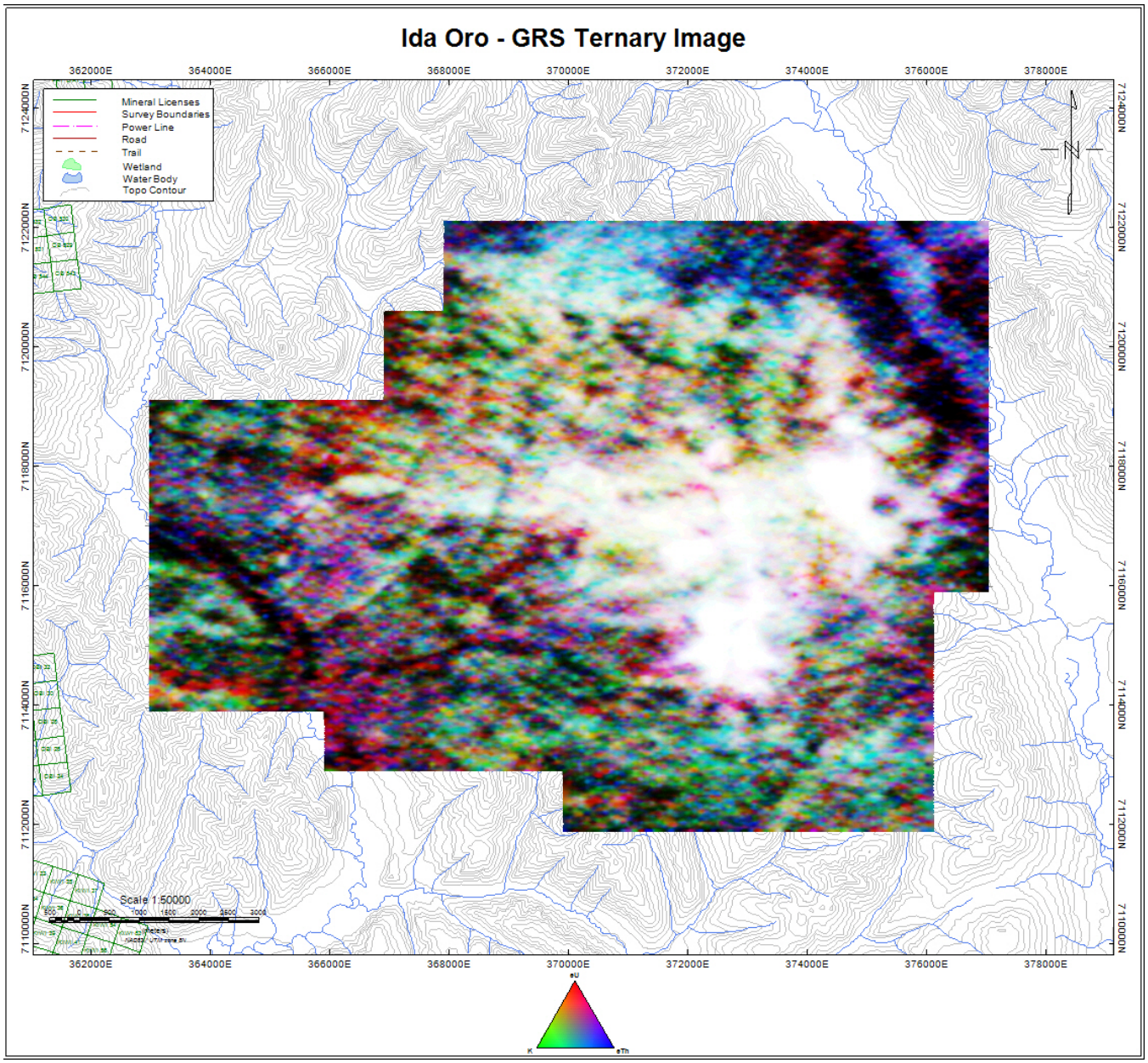


**Figure 20 – Color image of the radiometrics Ternary image over the Ida Oro survey area.**

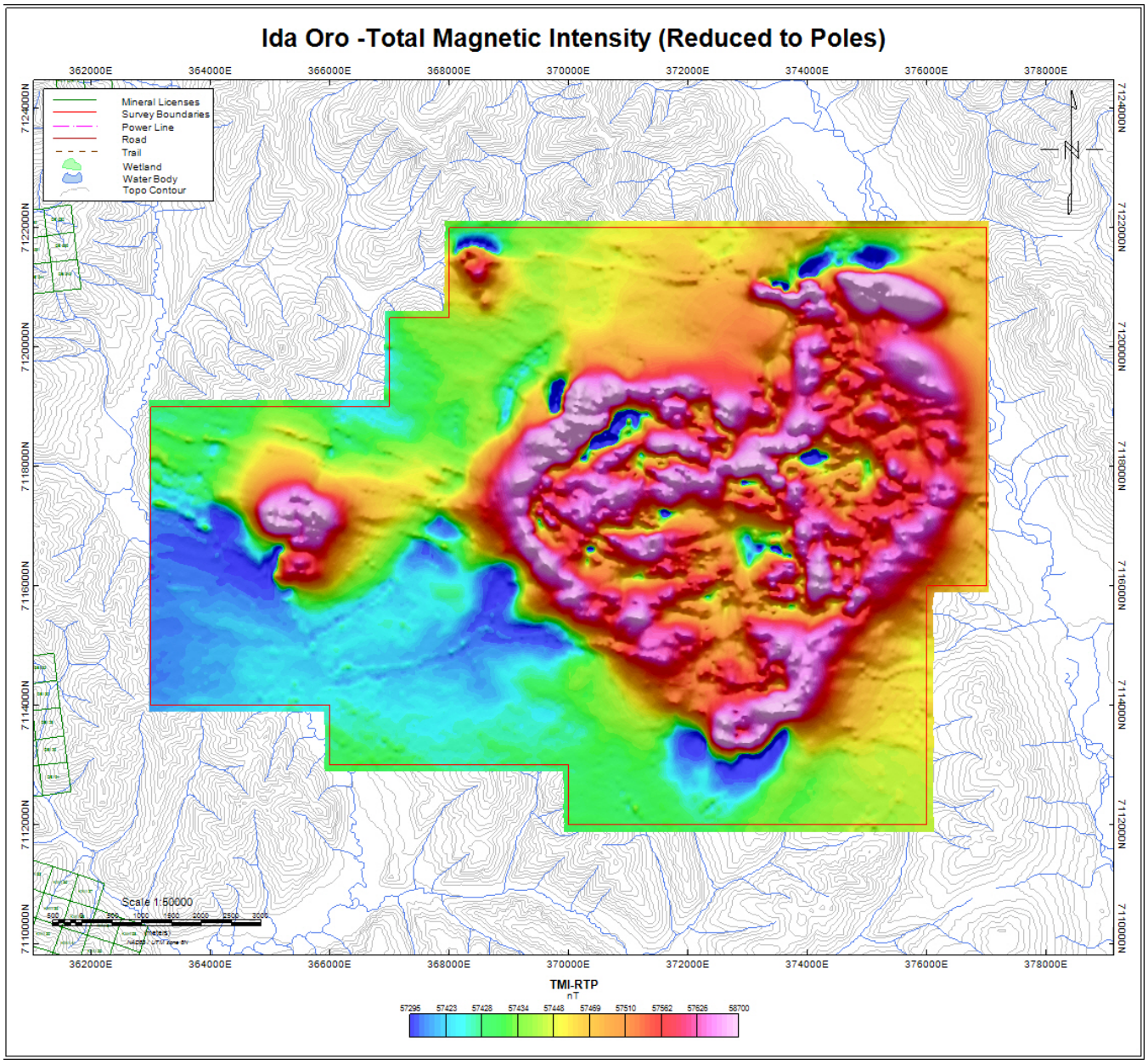


**Figure 21 – Shaded image of the TMI Reduced to Poles over the Ida Oro survey area.**

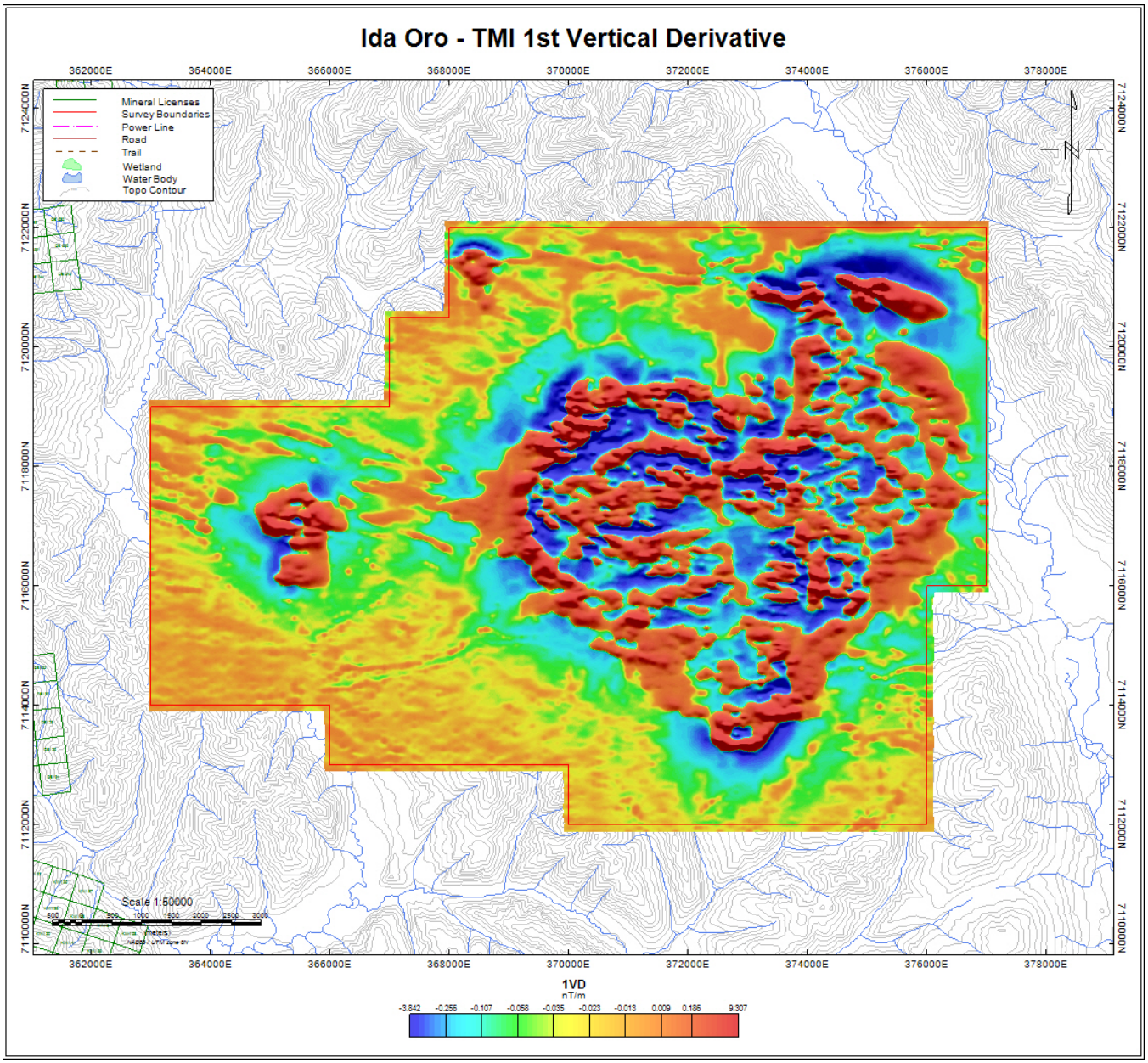


**Figure 22 – Shaded image of the TMI 1st Vertical Derivative over the Ida Oro survey area.**

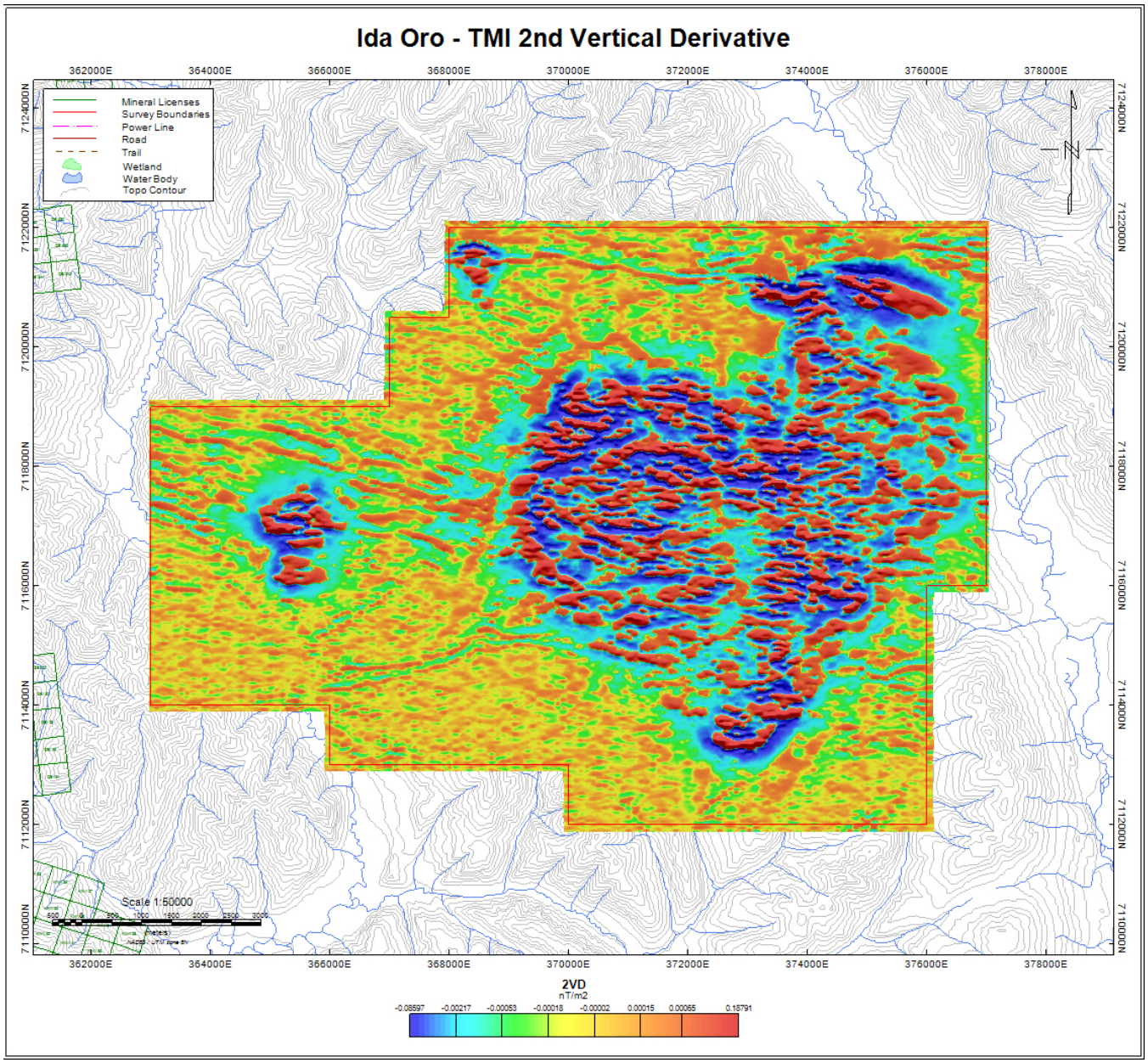


**Figure 23 – Shaded image of the TMI 2nd Vertical Derivative over the Ida Oro survey area.**

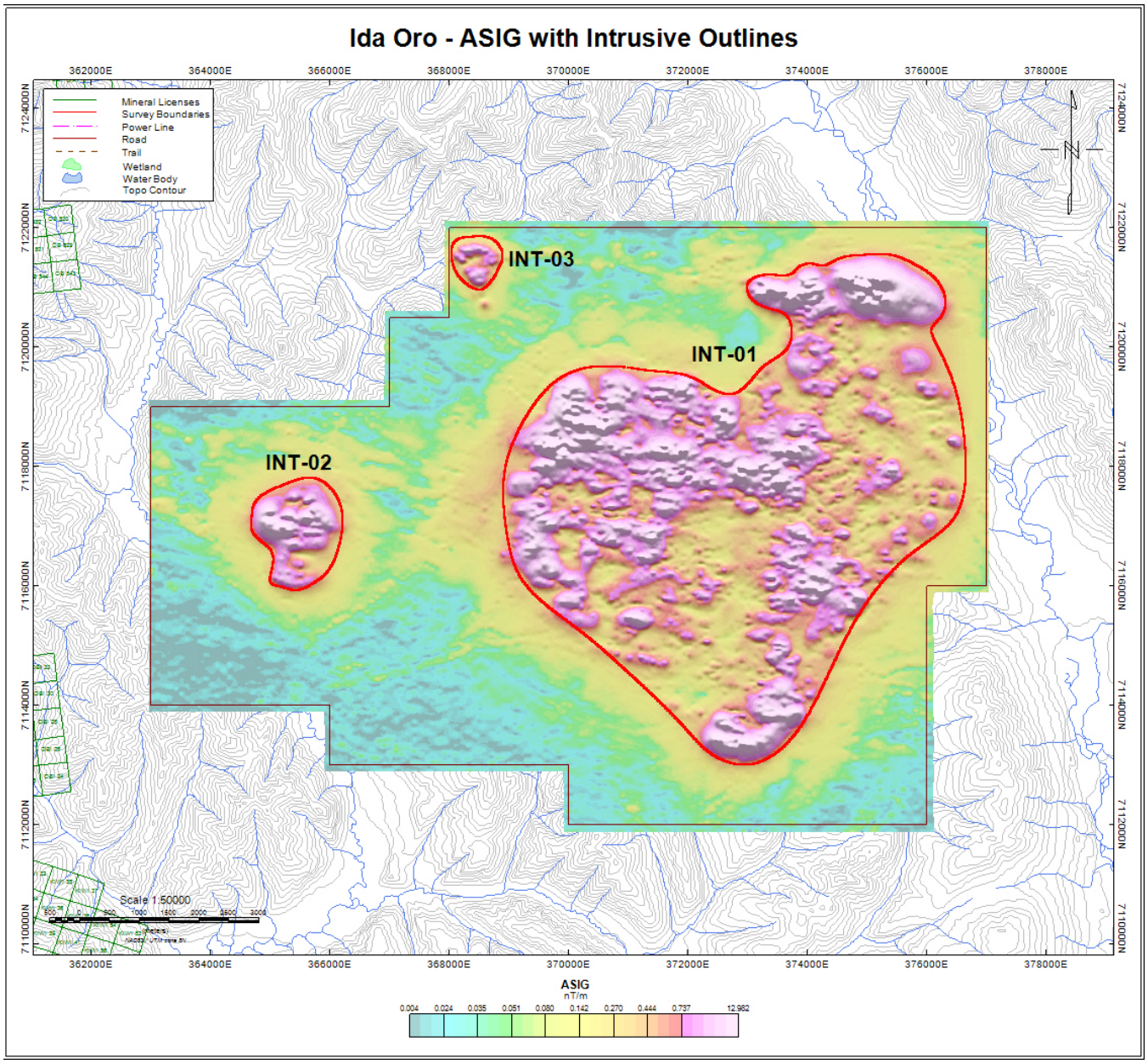


**Figure 24 – ASIG grid with intrusive groupings over the Ida Oro survey area.**

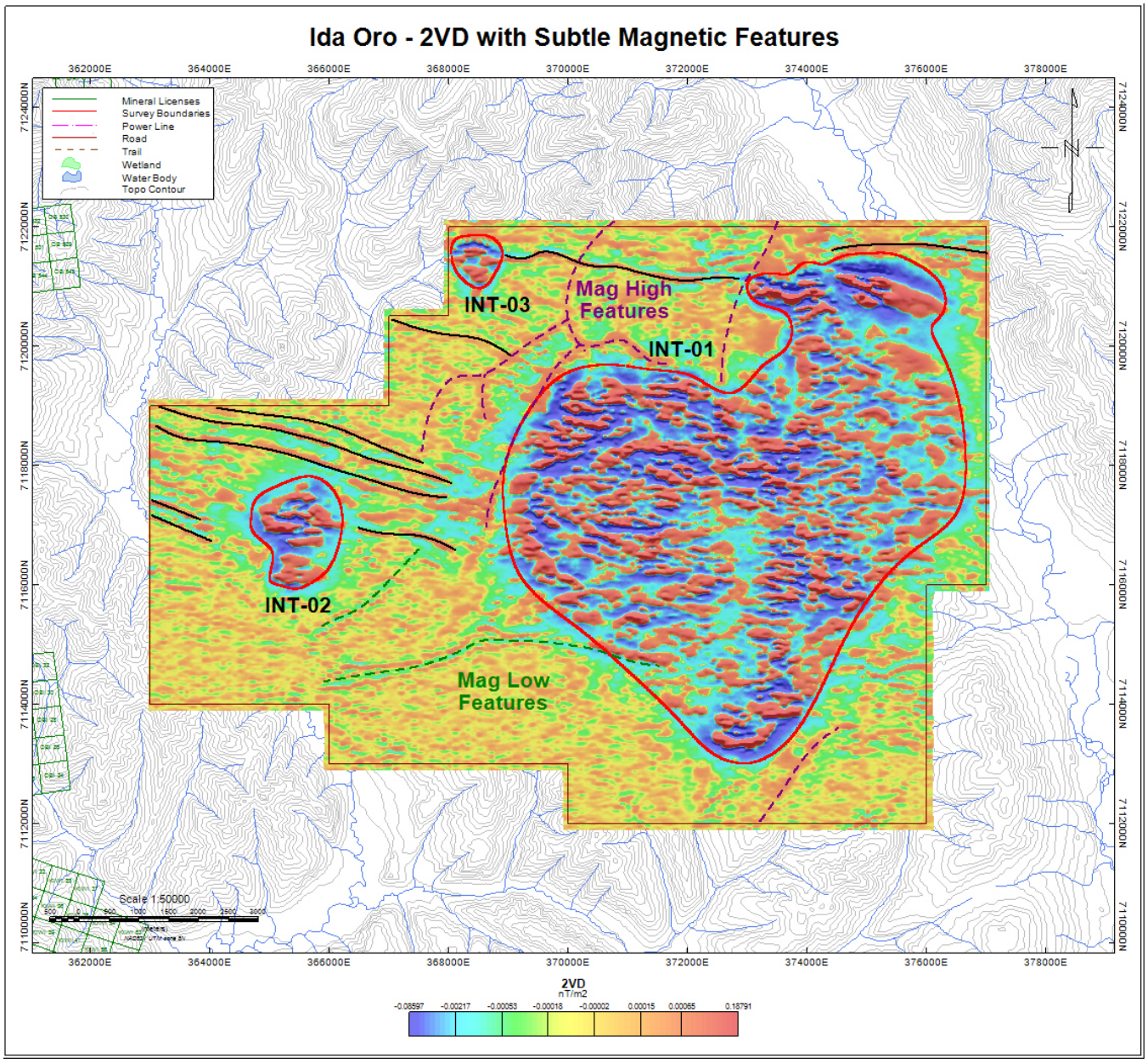


**Figure 25 – 2VD grid with subtle magnetic features throughout the survey area.**

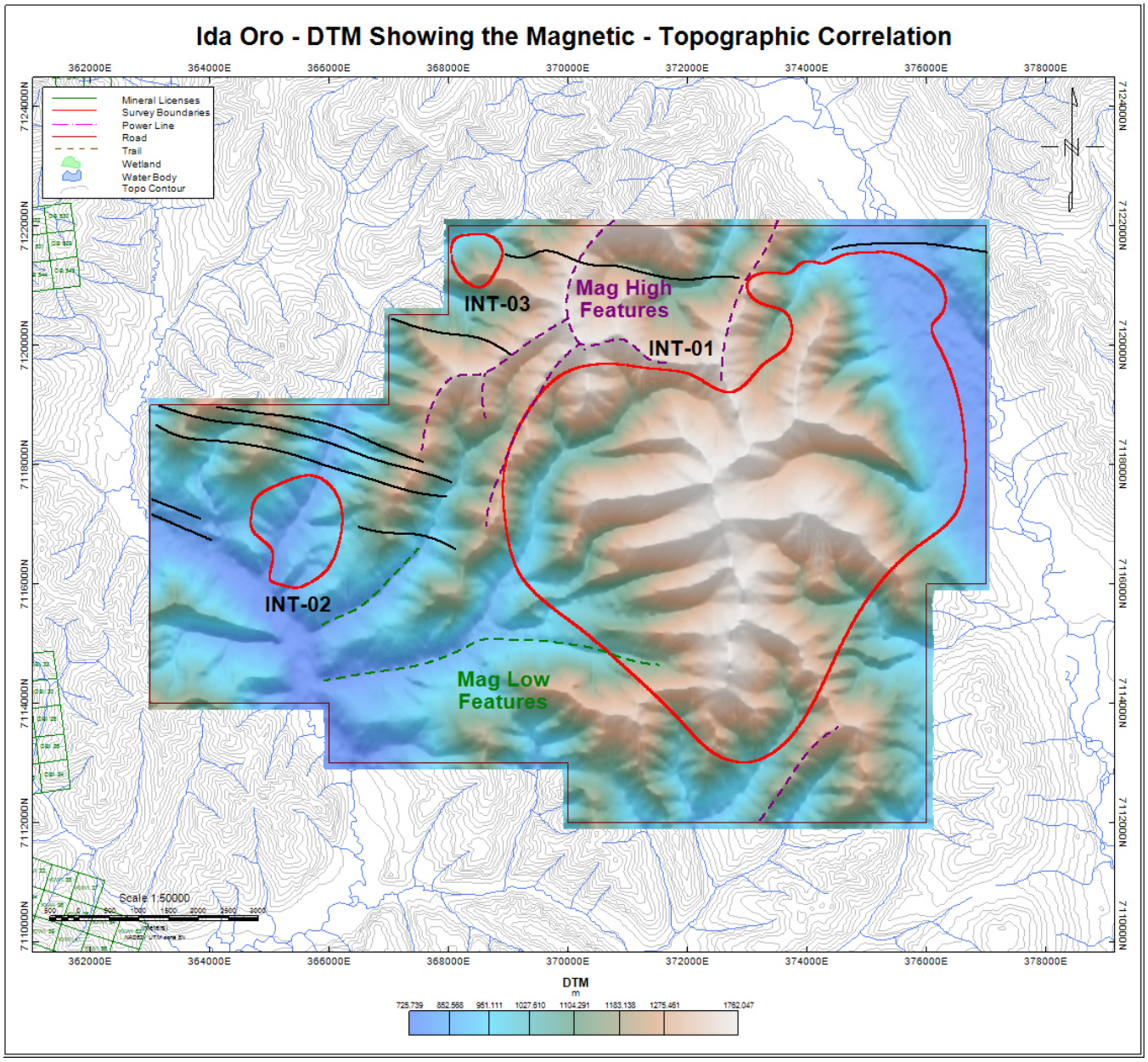


**Figure 26 – DTM grid showing the relationship between subtle magnetic features with the topography.**

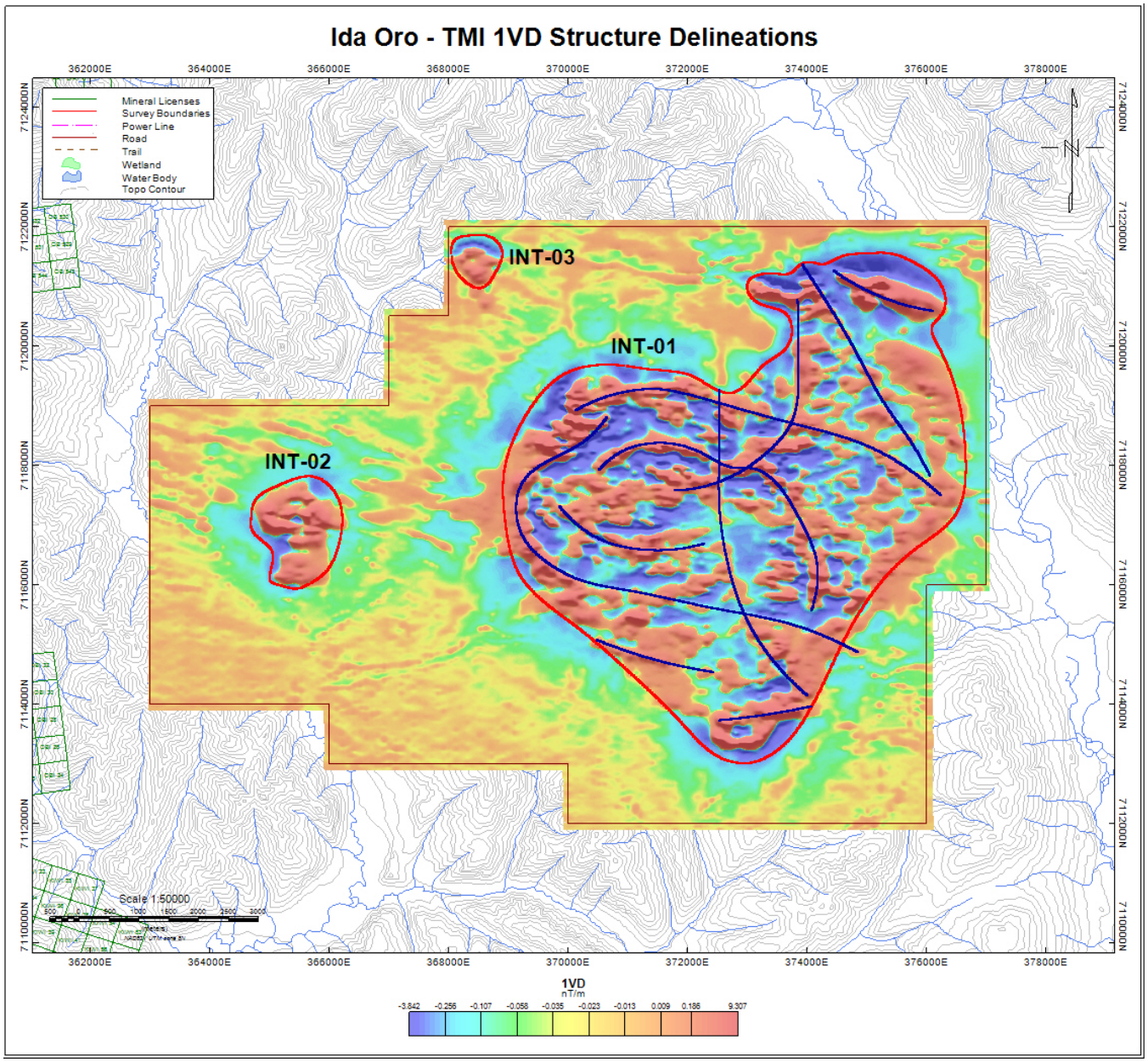


**Figure 27 – TMI 1VD grid showing the detailed intrusive fabric on INT-01.**

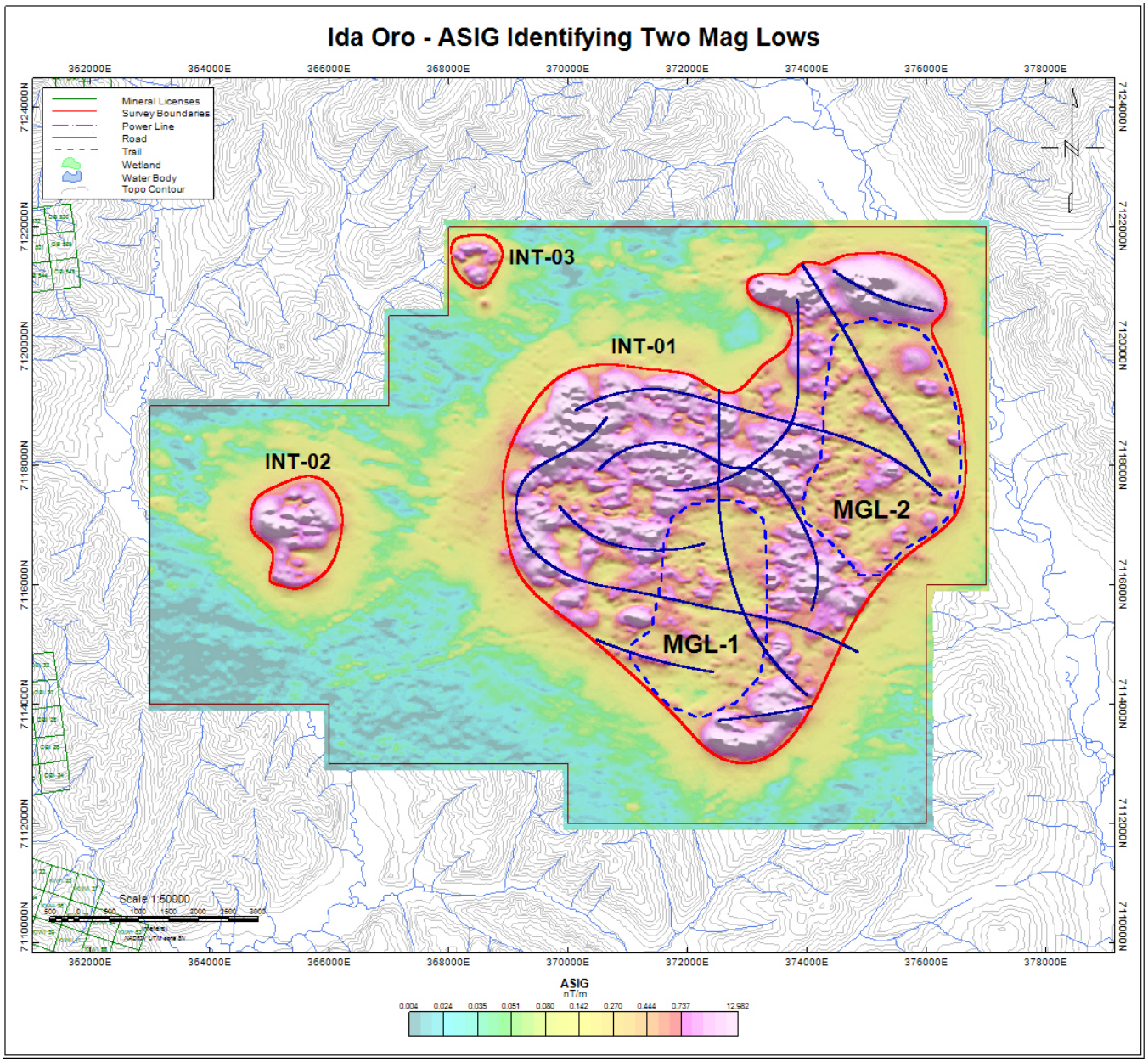


**Figure 28 – ASIG grid identifies two magnetic low zones within the intrusive body INT-01.**

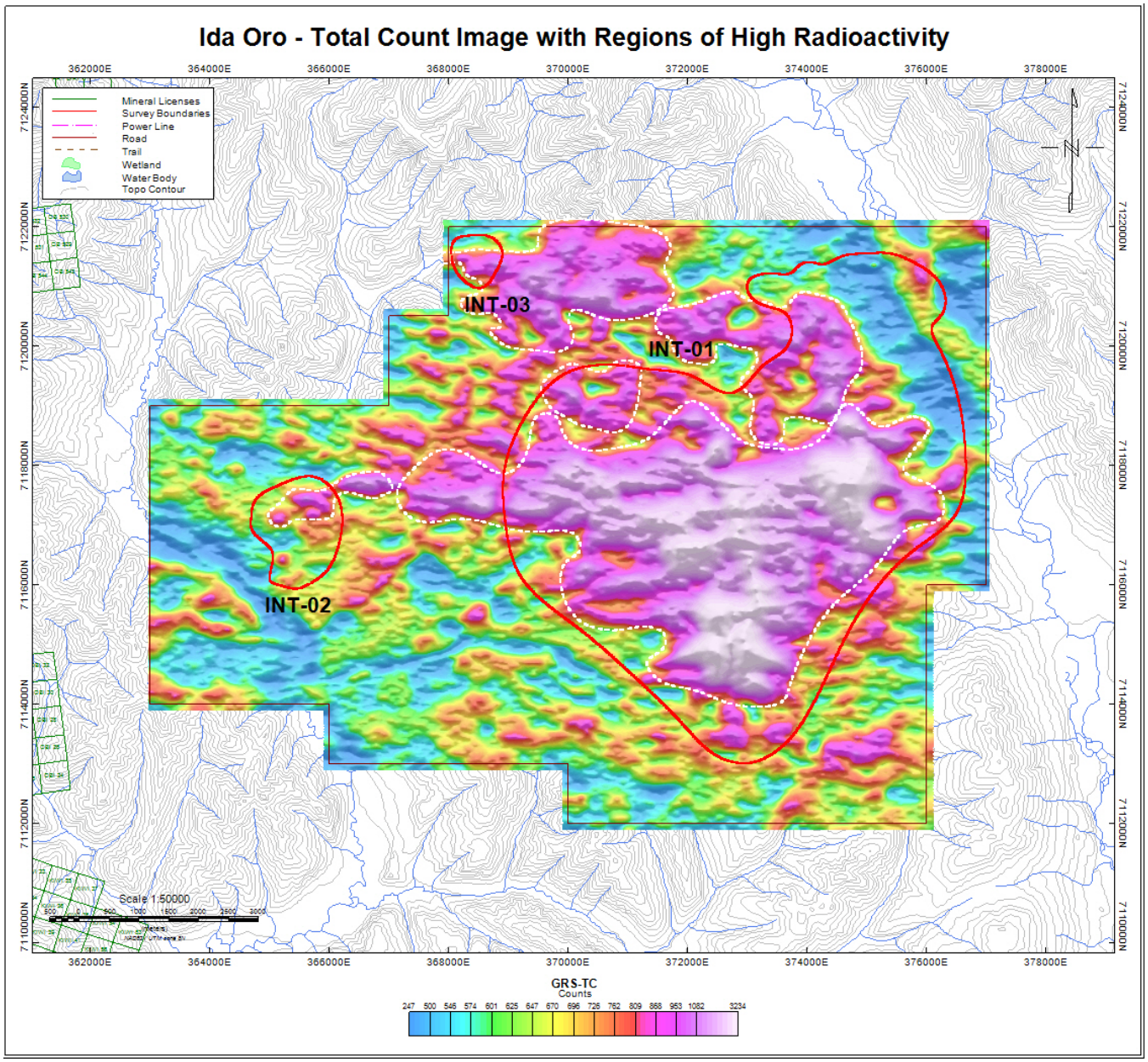


**Figure 29 – Total Count grid identifying regions of high radioactivity.**

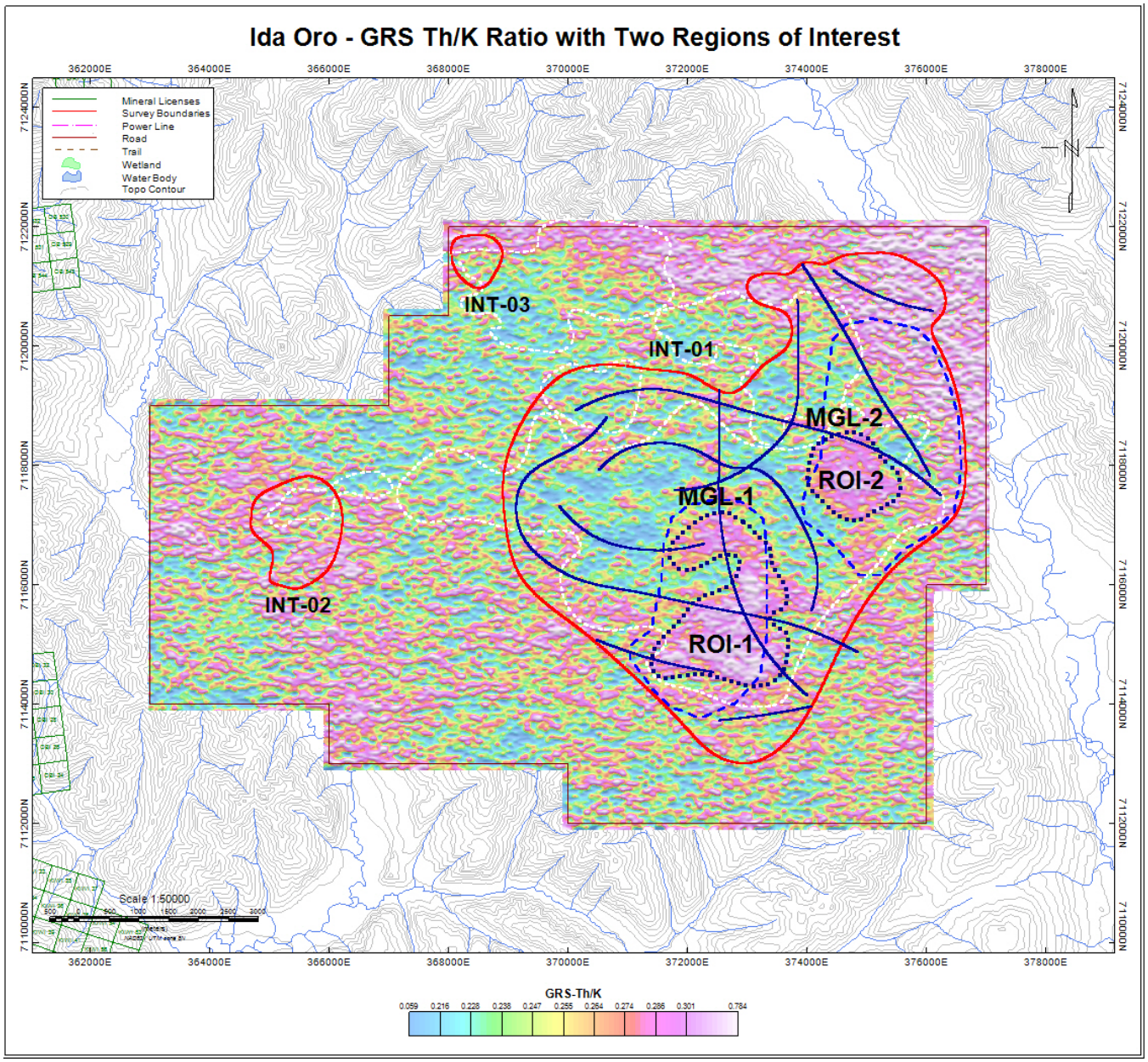


**Figure 30 – GRS Th/K Ratio grid with two regions, ROI-1 and ROI-2, of low ratio values.**

## APPENDIX A
## LIST OF SURVEY OUTLINE POINTS

The following survey polygon was produced by CMG and approved by the Client.

The Datum is NAD-83.

The Projection is UTM, Zone 8 North.

**Ida Oro**

| Easting | Northing |
|---|---|
| 363000 | 7119000 |
| 367000 | 7119000 |
| 367000 | 7120500 |
| 368000 | 7120500 |
| 368000 | 7122000 |
| 377000 | 7122000 |
| 377000 | 7116000 |
| 376000 | 7116000 |
| 376000 | 7112000 |
| 370000 | 7112000 |
| 370000 | 7113000 |
| 366000 | 7113000 |
| 366000 | 7114000 |
| 363000 | 7114000 |

## APPENDIX B
## LIST OF DATABASE COLUMNS (GEOSOFT GDB FORMAT)

| Channel Name | Description |
|---|---|
| x | X positional data (metres – NAD83, UTM Zone 8 north) |
| y | Y positional data (metres – NAD83, UTM Zone 8 north) |
| lon_wgs84 | Longitude data (degree – WGS84) |
| lat_wgs84 | Latitude data (degree – WGS84) |
| Lines | Line number |
| Flight | Flight number |
| Date | Flight date |
| gpstime | Coordinated Universal Time (UTC) measurement |
| gpsalt | Bird height above sea level (metres – ASL) |
| radalt | Bird height above ground (metres – AGL) |
| DTM | Digital Terrain Model (metres – ASL) |
| Basemag | Base station magnetic diurnal (nT) |
| Mag1 | Sensor 1 - Total Magnetic field data (nT) |
| Mag2 | Sensor 2 - Total Magnetic field data (nT) |
| Mag3 | Sensor 3 - Total Magnetic field data (nT) |
| TMI | Leveled Total Magnetic field data (nT) |
| ASIG | Magnetic analytical signal (nT) |
| MC_HMG | Measured Cross-Line Horizontal Magnetic Gradient (nT/m) |
| MI_HMG | Measured In-Line Horizontal Magnetic Gradient (nT/m) |
| M_VMG | Measured Vertical Magnetic Gradient (nT/m) |
| Temperature | Temperature record outside helicopter (ºC) |
| Pressure | Pressure reading outside helicopter (kPa) |
| Spec_GPSAlt | Altitude ASL record by the spectrometer GPS (m) |
| TC_Corr | Corrected GRS Total Counts (Counts) |
| pK | Percent Potassium (%) |
| eU | Equivalent Uranium (ppm) |
| eTh | Equivalent Thorium (ppm) |
| Th_K_Ratio | Thorium / Potassium Ratio (ppm/%) |
| U_K_Ratio | Uranium / Potassium Ratio (ppm/%) |
| U_Th_Ratio | Uranium / Thorium Ratio |